P C O I L S

Mathematical Models of Pulsed Tokamak Coil Systems for Studying Energy Requirement and Control Problems

J. Raeder

H. Gorenflo

IPP 4/184 November 1979

MAX-PLANCK-INSTITUT FÜR PLASMAPHYSIK

8046 GARCHING BEI MÜNCHEN

MAX-PLANCK-INSTITUT FÜR PLASMAPHYSIK

GARCHING BEI MÜNCHEN

P C O I L S

Mathematical Models of Pulsed Tokamak Coil Systems for Studying Energy Requirement and Control Problems

J. Raeder

H. Gorenflo

IPP 4/184 November 1979

Die nachstehende Arbeit wurde im Rahmen des Vertrages zwischen dem Max-Planck-Institut für Plasmaphysik und der Europäischen Atomgemeinschaft über die Zusammenarbeit auf dem Gebiete der Plasmaphysik durchgeführt.

A b s t r a c t

A mathematical model of the pulsed coil system of a tokamak which treats the plasma loop as a coil, too, is presented. The parameters involving this"plasma coil" may vary with time.

Both the equations describing the dynamics of the complete coil system and the formulae for calculating all system parameters are collected.

On this basis two concrete pulsed coil models are set up:

PCOILS 1 is a simple model, mainly for the purpose of quickly calculating the most relevant voltages, currents, and energies.

PCOILS 2 is a more involved model, mainly for studying control problems such as position and burn control.

The numerical solution of the sets of equations representing PCOILS 1 and PCOILS 2, and the continuous checking of the energy balance of the system during the solution is described. In connection with PCOILS 2 the passive stabilization of the plasma position by chamber wall currents is treated in terms of the mutual inductance of the plasma loop and dipole chamber currents.

Finally, the PCOILS 1 and PCOILS 2 models are applied to the current rise phase of the ASDEX divertor tokamak and to the compression phase of the ZEPHYR tokamak ignition experiment.

Contents

1. Introduction

Our aim is to set up mathematical models of poloidal field coil systems for tokamaks. These models will be used in the IPP Systems Studies Group for both the investigation of fusion reactor energy balances and studies of position and burn control.

Figure 1 schematically shows the coil systems treated and the coordinate system.

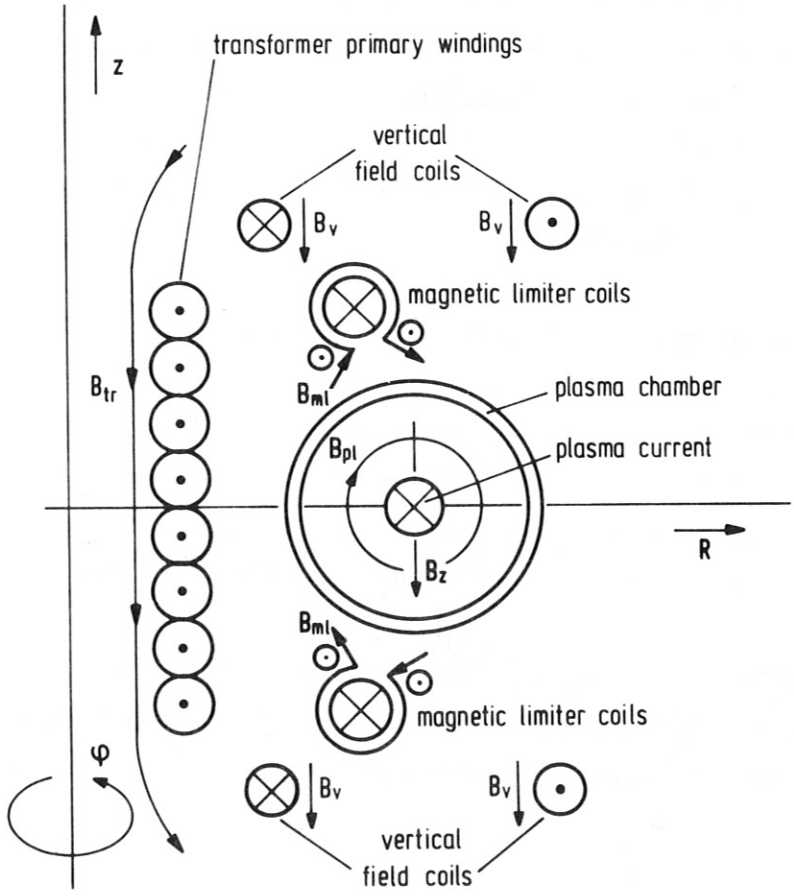

Fig. 1

As a basis for the models we have to collect the equations to be used and derive simple analytical formulae for the inductances and resistances of the various coils and for the poloidal magnetic field components produced by the coil currents.

Because of the numerous components involved it is necessary to restrict the number of parameters characterizing an individual component. This calls for an approach which emphasizes the modelling of the mutual relations but does not strive for utmost precision. This goal can be achieved by calculating the inductances and other magnetic circuit parameters from approximate solutions of the Grad-Shafranov equation describing the various poloidal field coils of a tokamak. As is well known for the case of a plasma ring, the simplifications are mainly due to assuming ideal toroidal symmetry and small values of the inverse aspect ratio. The errors mainly stem from extrapolating the results to appreciable values of the inverse aspect ratio. The advantage of the method lies in the possibility of characterizing each poloidal coil system by only two or three parameters.

On this basis we shall set up the two coil models, PCOILS 1 (Pulsed Coils 1) and PCOILS 2.

PCOILS 1 will be used in our fusion power plant model SISYFUS mainly for energy balance studies. Because such systems studies call for a very large number of computer runs we have to keep the computing time of PCOILS 1 as short as possible. This is mainly achieved by introducing various simplifications which, in turn, omit the possibility of treating fast processes such as fast compression or position control.

The study of such processes is possible by using the PCOILS 2 model, which is considerably more involved. In PCOILS 2 the main emphasis is put on consistent treatment of changes in plasma position and poloidal fluxes.

2. Pulsed coil system of a tokamak

A tokamak comprises various poloidal coils mutually coupled by their magnetic fields. We restrict ourselves to the following coils:

- plasma loop,
- primary transformer winding,
- vertical field coils,
- magnetic limiter coils,
- plasma chamber.

The plasma loop is thus treated as a coil.

What we call "magnetic limiter coils" may also be interpreted as, for example, "plasma shaping coils" in the context of a tokamak plasma with specifically shaped minor cross-section.

The plasma chamber current is represented by its Fourier components with respect to the poloidal angle θ up to second order. This means that the mean value of an induced chamber current, its dipole and its quadrupole component is taken into account.

The complete coil system thus comprises seven coils, which are shown schematically in Fig. 2 together with the currents, voltages, and resistances involved (the resistances R_i are named R_{0i} in the text).

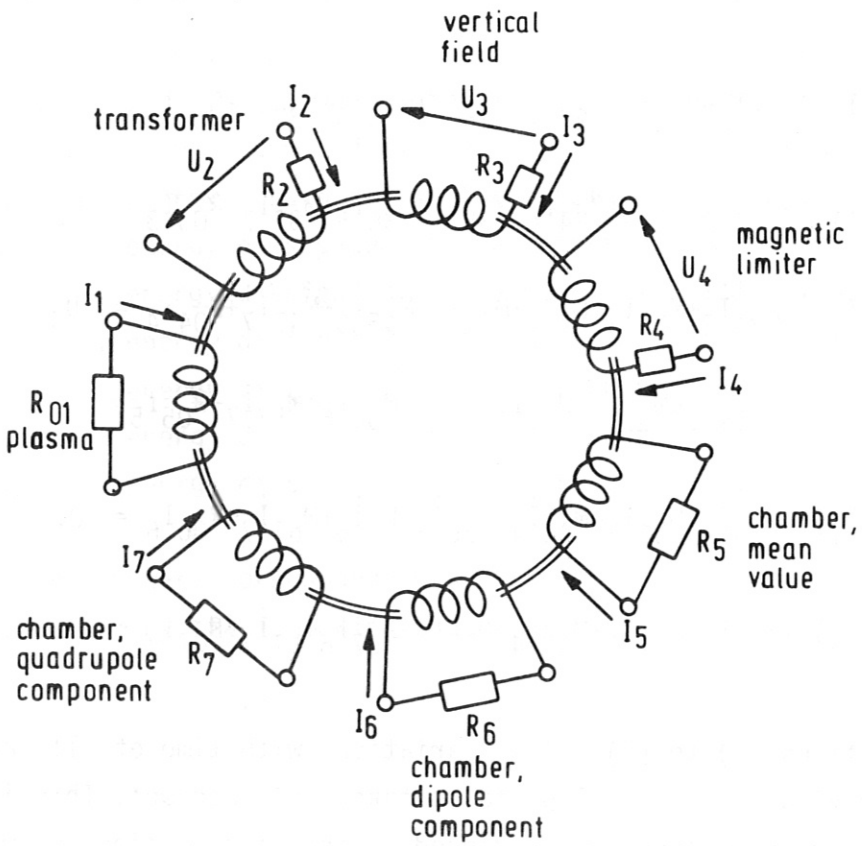

Fig. 2

To avoid complicated indexing in the circuit equations, the coils and the corresponding currents, voltages, and resistances are numbered according to the following scheme:

plasma	pl	1
transformer	tr	2
vertical field	v	3
magnetic limiter	ml	4
chamber, mean value	c0	5
chamber, dipole component	c1	6
chamber, quadrupole component	c2	7

3. Set of equations used

3.1 Electric circuit equations

The currents and voltages of the various coils are interrelated by the following set of electric circuit equations:

$$(L_1 I_1)^{\cdot}+(M_{12} I_2)^{\cdot}+(M_{13} I_3)^{\cdot}+(M_{14} I_4)^{\cdot}+(M_{15} I_5)^{\cdot}+(M_{16} I_6)^{\cdot}+(M_{17} I_7)^{\cdot}+ R_{01} I_1 = 0, \quad (1)$$

$$(M_{12} I_1)^{\cdot}+L_2 \dot{I}_2+M_{23} \dot{I}_3+M_{24} \dot{I}_4+M_{25} \dot{I}_5+M_{26} \dot{I}_6+M_{27} \dot{I}_7+R_{02} I_2 = U_2, \quad (2)$$

$$(M_{13} I_1)^{\cdot}+M_{23} \dot{I}_2+L_3 \dot{I}_3+M_{34} \dot{I}_4+M_{35} \dot{I}_5+M_{36} \dot{I}_6+M_{37} \dot{I}_7+R_{03} I_3 = U_3, \quad (3)$$

$$(M_{14} I_1)^{\cdot}+M_{24} \dot{I}_2+M_{34} \dot{I}_3+L_4 \dot{I}_4+M_{45} \dot{I}_5+M_{46} \dot{I}_6+M_{47} \dot{I}_7+R_{04} I_4 = U_4, \quad (4)$$

$$(M_{15} I_1)^{\cdot}+ M_{25} \dot{I}_2+M_{35} \dot{I}_3+M_{45} \dot{I}_4+L_5 \dot{I}_5+M_{56} \dot{I}_6+M_{57} \dot{I}_7+R_{05} I_5= U_5, \quad (5)$$

$$(M_{16} I_1)^{\cdot}+M_{26} \dot{I}_2+M_{36} \dot{I}_3+M_{46} \dot{I}_4+M_{56} \dot{I}_5+L_6 \dot{I}_6+M_{67} \dot{I}_7+R_{06} I_6 = 0, \quad (6)$$

$$(M_{17} I_1)^{\cdot}+M_{27} \dot{I}_2+M_{37} \dot{I}_3+M_{47} \dot{I}_4+M_{57} \dot{I}_5+M_{67} \dot{I}_6+L_7 \dot{I}_7+R_{07} I_7 = 0. \quad (7)$$

Equations (1) to (7) allow variations with time of all inductances involving the plasma loop to be taken into account. This is necessary because these inductances depend on the plasma major and minor radii R_1 and r_1 and partly also on the plasma internal inductance l_i,

the poloidal beta β_p, and the plasma elongation e_1, which may all vary with time.

The resistances R_{oa} ("o" for "ohmic")may also be functions of time. For the plasma this is due to the variations of plasma temperature and plasma geometrical data, while for the remaining coils such variations may be caused by ohmic heating of normal conducting coils or by the dynamic resistivity of superconducting coils.

The voltage U_5 is not applied from outside but develops across the poloidal slits which may be used to suppress an induced average toroidal current I_5 in the chamber walls (or in the liner).

3.2 Equations for the various electric powers

During tokamak operation the power supplies with the voltages U_2 (transformer), U_3 (vertical field), and U_4 (magnetic limiter) deliver energy to (or get energy back from) the coil system. Part of the energy supplied is dissipated in the coils. To describe these processes, we calculate the following energies:

E_1 . . . energy supplied by the transformer power supply,
E_2 . . . energy supplied by the vertical field power supply,
E_3 . . . energy supplied by the magnetic limiter power supply,
E_4 . . . energy dissipated in the plasma,
E_5 . . . energy dissipated in the transformer windings,
E_6 . . . energy dissipated in the vertical field windings,
E_7 . . . energy dissipated in the magnetic limiter windings,
E_8 . . . energy dissipated by chamber current I_5,
E_9 . . . energy dissipated by chamber current I_6,
E_{10} . . energy dissipated by chamber current I_7.

The electric powers corresponding to the energies of the above list are determined by the following equations:

$$P_1 = dE_1/dt = U_2 I_2, \tag{8}$$

$$P_2 = dE_2/dt = U_3 I_3, \tag{9}$$

$$P_3 = dE_3/dt = U_4 I_4, \tag{10}$$

$$P_4 = dE_4/dt = I_1^2 R_{01}, \tag{11}$$

$$P_5 = dE_5/dt = I_2^2 R_{02}, \tag{12}$$

$$P_6 = dE_6/dt = I_3^2 R_{03}, \tag{13}$$

$$P_7 = dE_7/dt = I_4^2 R_{04}, \tag{14}$$

$$P_8 = dE_8/dt = I_5^2 R_{05}, \tag{15}$$

$$P_9 = dE_9/dt = I_6^2 R_{06}, \tag{16}$$

$$P_{10} = dE_{10}/dt = I_7^2 R_{07}. \tag{17}$$

3.3 Vertical magnetic field produced at the plasma centre by the various coil currents

We describe the vertical magnetic field B_{a1} produced at the plasma centre $R = R_1$ by a current I_a flowing in a poloidal coil "a" by

$$B_{a1} = \nu_{a1} I_a, \tag{18}$$

where ν_{a1} is a parameter determined solely by geometry (s. Sec. 4.2).

The fact that toroidal currents in the coils are induced during a dynamic phase of the tokamak discharge leads to a delay in the propagation of the poloidal magnetic fields. The most important of these is the delay of the field produced by the vertical field current I_3 owing to the dipole component I_6 of the chamber current.

Another feature of the same origin is the induction of chamber currents by shifts of the plasma centre which reflect into changes of the mutual inductances between plasma and chamber components. The induction of a dipole current I_6 in the chamber by a plasma shift, for example, leads to the well known plasma equilibrium on the L/R time scale of the chamber.

The effects described above are properly described by the circuit equations (1) to (7) together with the equations of type (18) for the vertical magnetic fields. Important in this context is the fact that the mutual inductances involving the plasma loop depend on R_1.

For mathematical convenience we shall use the differentiated form of eq. (18)

$$\dot{B}_{a1} = (\nu_{a1} I_a)^{\cdot} \quad . \tag{19}$$

3.4 Equation for the major radius R_1 of the plasma column

The equation of motion for a large aspect ratio toroidal plasma loop with circular minor cross-section is given by

$$m_{pl} \ddot{R}_1 - 2\pi R_1 I_1 B_z - \mu_o I_1^2/2 \cdot (\ell n 8R_1/r_1 + \lambda_1 - 1/2) = 0 \tag{20}$$

with

$$\lambda_1 = \beta_p + \ell_i/2 - 1, \tag{21}$$

$$\ell_i = 2L_{1i}/\mu_o R_1 \tag{22}$$

(m_{pl} = total plasma mass, R_1 = major plasma radius, r_1 = minor plasma radius I_1 = plasma current, β_p = poloidal plasma β, L_{1i} = internal plasma inductance).

For investigations where high-frequency MHD oscillation do not play a significant role, plasma inertia may be neglected by setting m_{pl} equal to zero. The result thus following from eq. (20) is the usual equation for the equilibrium vertical field B_z

$$B_z = -\mu_o I_1/4\pi R_1 \cdot (\ell n\ 8R_1/r_1 + \lambda_1 - 1/2). \tag{23}$$

To be consistent with the notation used in Sec. 3.3, we rewrite eq. (23) in the following form:

$$B_z = \nu_1 I_1 \tag{24}$$

with

$$\nu_1 = -\mu_o/4\pi R_1.(\ell n\ 8R_1/r_1 + \lambda_1 - 1/2). \qquad (25)$$

Obviously B_z is not the field produced by the plasma current I_1 at $R = R_1$ but is the field necessary to keep the plasma in equilibrium at $R = R_1$ for the specified plasma parameters r_1, β_p, and ℓ_i.

To incorporate eq. (23) into our system of differential equations, we differentiate it with respect to time and interpret it as the equation governing the time evolution of R_1:

$$\dot{R}_1 B_z + R_1\dot{B}_z + \mu_o I_1/4\pi.(\dot{R}_1/R_1 - r_1/r_1 + \dot{\lambda}_1) - \nu_1 R_1 \dot{I}_1 = 0 . \qquad (26)$$

3.5 Equation for the plasma minor radius r_1

We define the circle enclosing the plasma current I_1 by $r = r_1$.

The simplest definition of r_1 is the assumption that $r = r_1$ encircles the same toroidal magnetic flux Φ_t at any instant in time. This condition holds for adiabatic variations or if, for example, a rail limiter is always tangential to the same flux surface when the plasma moves.

From the approximation

$$\Phi_t = \pi r_1^2 B_t \qquad (27)$$

[$B_t = B_t\ (R=R_1, r=0)$ = toroidal magnetic field at the plasma centre]

and

$$B_t.R_1 = \text{const} \qquad (28)$$

we get, if $d\Phi_t/dt = 0$,

$$\dot{r}_1 - 1/2.r_1\dot{R}_1/R_1 = 0 . \qquad (29)$$

If variations of r_1 due to external intervention (e.g. a moving limiter) or due to plasma diffusion (e.g. if no limiter is present) have to be described, the apppropriate terms have to be used instead of the zero on the right-hand side of eq. (29).

3.6 Equation for the safety factor q at the plasma edge $r = r_1$.

The safety factor $q = q(r=r_1)$ of a plasma with circular minor cross-section to lowest order in r_1/R_1 is given by

$$q = \frac{2\pi B_t R_1}{\mu_o} \cdot \frac{r_1^2}{I_1 R_1^2} \cdot \tag{30}$$

By using the relation (28) we get from eq. (30) upon differentiation

$$\frac{\dot{I}_1}{I_1} + 2\frac{\dot{R}_1}{R_1} - 2\frac{\dot{r}_1}{r_1} = -\frac{\dot{q}}{q} \cdot \tag{31}$$

At least during non-turbulent phases of the plasma, q/q_o varies only slowly with time (q_o = safety factor on the plasma axis $r = 0$). The associated time scale is the L_{1i}/R time of the plasma (L_{1i} = internal plasma inductance). In special situations such as fast plasma compression I_1, R_1, and r_1 may vary rapidly but the fast changes have to cancel in order to satisfy eq. (31). The prescription of $\dot{q}$ instead of $\dot{I}_1$ is therefore physically reasonable if fast processes (i.e. burn control cycles) have to be treated. The ambiguous prescription of $\dot{I}_1$ in such situations would lead to unphysical flux changes with the associated high induced voltages occurring in the coil systems.

4. Collection of formulae for the circuit parameters

4.1 Inductances

The calculation of the self and mutual inductances is based on the flux functions associated with the current density distributions in the various coils.

For the flux function Ψ_{pl} of the plasma the formula given in /1/ was used.

The flux functions of the transformer, vertical field coils and the three chamber current components (average, dipole, quadrupole) were calculated according to a procedure given in /2/. The associated calculations are described in /3/. For these calculations a poloidal coil system "a" is modelled by a shell with cylindrical minor cross-section of radius r_a carrying a toroidal line current density $i_a(\theta)$. This current density, in general, is a function of the poloidal angle θ in order to produce the desired poloidal field B_{pa}. The arrangemend described above is schematically shown in Fig. 3.

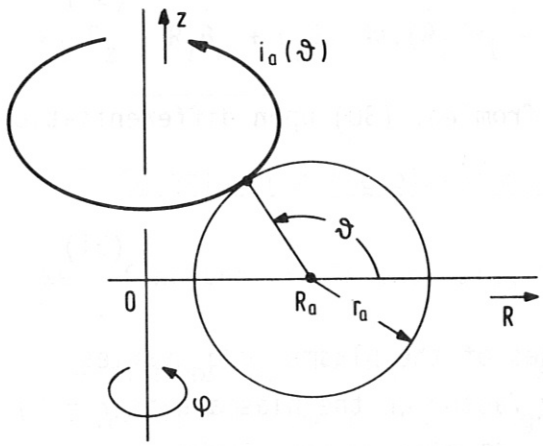

Fig. 3

We shall also apply the results calculated for coils with circular minor cross-sections to coils with cross-sections elongated in the z-direction. This will be done by heuristically inserting an effective minor radius in the leading (logarithmic) terms of the various inductances. This effective radius r_{ae} is given by

$$r_{ae} = (r_a z_a)^{1/2} \qquad (32)$$

with r_a = radial half-width and z_a = half-height of the minor cross-section (see Fig. 4). The procedure of using r_{ae} instead of r_a may be justified by comparison with the proposal made in /4/ to use the equivalent minor radius $r_{ae} = 1/2\ (r_a + z_a)$ for the case of a homogeneous current distribution in a conductor with elliptic cross-section (semi-axes r_a and z_a). This proposal is based on the concept of the "geometric mean distance" of a cross-section from itself. Whether one uses $(r_a z_z)^{1/2}$ or $1/2.(r_a + z_a)$ is of minor importance for the moderate elongations z_a/r_a we have to deal with ($z_a/r_a \lesssim 2$). Whether the minor cross-section is elliptical (as schematically assumed in Fig. 4) or, for example, D-shaped, does not have to be specified within the rough approximation we use.

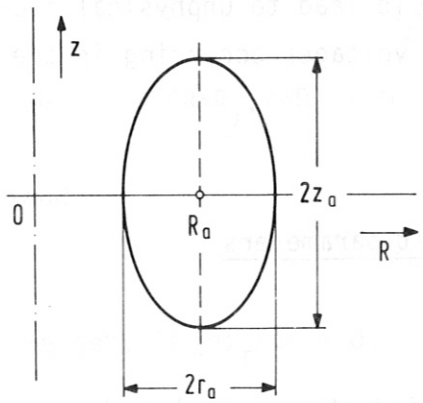

Fig. 4

The elongation of a minor coil cross-section is described by the parameter

$$e_a = z_a/r_a \ , \tag{33}$$

while the toroidicity ε_a of the coil is given by the inverse aspect ratio A_a:

$$\varepsilon_a = 1/A_a = r_a/R_a \ . \tag{34}$$

For circular coils the formulae for the inductances were originally computed by including terms up to first order in ε_a.

Second-order contributions were estimated by using the exact values for the inductance of a toroidal, current-carrying shell given in /5/.

The θ-dependence of the surface current distributions was taken into account up to the second Fourier component.

Inherent to our thin-shell approximation is the neglect of the time τ_{ai} necessary to build up the current density profile inside the conductor compared with the external L/R time τ_{ae} of the coil. The latter is dominated by the external inductance, whereas the former is determined by the internal inductance.

These times are approximately given by /6/, /7/:

$$\tau_{ai} = \frac{1}{\pi^2} \ \mu_o \sigma_a \, d_a^2 \ , \tag{35}$$

$$\tau_{ae} = \frac{1}{2} \ \mu_o \sigma_a r_a \, d_a \tag{36}$$

(σ_a = electrical conductivity of the material of coil "a", d_a = typical lateral dimension of coil "a" as, for example, the wall thickness of the plasma chamber).

Equations (35) and (36) show that the delay time

$$\tau_a = \tau_{ae} + \tau_{ai} \tag{37}$$

caused by a coil system or the plasma chamber is dominated by τ_{ae}, which is larger than τ_{ai} at least by a factor of at least r_a/d_a. In practice

this factor is of the order 10^2, which in turn means that the thin-shell approximation will introduce only small errors when applied to dynamic phases of tokamak discharges.

The mutual inductances involving a magnetic limiter coil triple as shown in Fig. 5 were calculated by idealizing the coils to infinitely thin current-carrying rings. Only for the calculation of the self-inductance of the triple we had to take the lateral dimension (i.e. the radius r_{qz} of the central coil) into account.

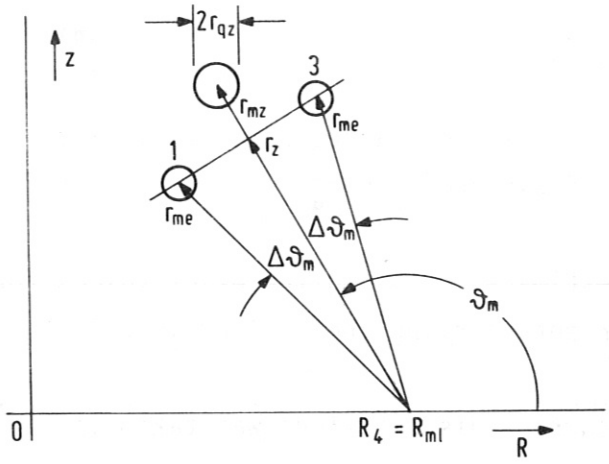

Fig. 5

Table 1 contains the functions ℓ_a and m_{ab}, which are related to the self and mutual inductances L_a and M_{ab} by

$$\ell_a = L_a/N_a^2 \,, \tag{38}$$

$$m_{ab} = M_{ab}/N_aN_b \tag{39}$$

(N_a = number of turns of coil "a", N_b = number of turns of coil "b").

Because there is a certain ambiguity in defining the various N_a they are specified as follows:

$N_1 = 1$,
N_2 = total number of transformer primary windings,
N_3 = half the number of turns of the total vertical field coil,
N_4 = number of turns of the central coil of one triple,
$N_5 = 1$,
$N_6 = 1$,
$N_7 = 1$.

It is obvious that the numbers of turns N_1, N_5, N_6 , and N_7 are physically unity. N_3 is chosen because the total vertical field coil is composed of two blocks, each carrying the same amount of ampere-turns which, however, are opposite in sign. The central magnetic limiter coil also carries the same amount of ampere-turns as the two excentric coils

together. Again these ampere-turns are opposite in sign to those of the central coil.

The ℓ_a and m_{ab} are the appropriate inductances when ampere-turns instead of currents and voltages per turn instead of voltages are used in the circuit equations.

Table 1 gives only half of the m_{ab}'s because of the symmetry relation

$$m_{ab} = m_{ba} \ . \tag{40}$$

The normalized internal inductance ℓ_i which occurs in the plasma inductance L_1 is determined by the radial profile of the poloidal field $B_{1\theta}$ produced by the plasma current I_1. For the calculation of ℓ_i one can use the magnetic energy stored inside the plasma. To lowest order in r/R_1 the field $B_{1\theta}$ does not depend on θ and is given by

$$B_{1\theta}(r) = \frac{\mu_o}{r} \int_o^r j_1(r')\, r'dr' \ , \tag{41}$$

$j_1(r)$ = radial profile of the toroidal plasma current density. By using the definition (22) of ℓ_i together with the formula for the stored magnetic energy

$$L_{1i}\, I_1^2 = \int_{(V)} B_{1\theta}^2 / \mu_o . dV \tag{42}$$

(V = plasma volume) we get for ℓ_i

$$\ell_i = 2 \int_o^{r_1} 1/r.dr \Big[\int_o^r j_1(r')r'dr' \Big]^2 / \Big[\int_o^{r_1} j_1(r)rdr \Big]^2 \ . \tag{43}$$

To demonstrate the dependence of ℓ_i on the peakedness of the current density profile, we evaluated eq. (43) for the distribution

$$j_1(r) = j_1(o)\, [1-(r/r_1)^2]^n \tag{44}$$

as a function of n. Figure 6 shows $\ell_i(n)$. Present-day experiments such as PLT show rather peaked T_e-profiles which via $\sigma \sim T_e^{3/2}$ should lead

$l_1 = \mu_o R_1 (\ln 8R_1/r_{1e} - 2 + l_i/2)(1-\varepsilon_1^2)$

$m_{12} = \mu_o R_2 (\ln 8R_2/r_{2e} - 2)(1-\varepsilon_2^2)$

$m_{13} = \mu_o \pi r_3 \cdot (R_1/R_3)/4k \cdot [(\ln 8R_1/r_{3e} - 1) + (r_1/r_3)^2 \cdot (R_3/R_1) \cdot (\lambda_1 + 1/2) + 2R_3/r_3^2 \cdot (R_1 - R_3)]$

$m_{14} = \mu_o R_1 (1 + 1/2 \cdot \varepsilon_{mz} \cos\delta_m) \cdot \ln \varepsilon_{me}/\varepsilon_{mz}$; $\varepsilon_{mz} = r_{mz}/R_4$, $\varepsilon_{me} = r_{me}/R_4$

$m_{15} = \mu_o R_5 (\ln 8R_5/r_{5e} - 2)(1-\varepsilon_5^2)$

$m_{16} = \mu_o \pi r_5/4 \cdot (R_1/R_5) \cdot [(\ln 8R_1/r_{5e} - 1) + (r_1/r_5)^2 \cdot (R_5/R_1) \cdot (\lambda_1 + 1/2) + 2R_5/r_5^2 \cdot (R_1 - R_5)]$

$m_{17} = 0$

$l_2 = \mu_o R_2 (\ln 8R_2/r_{2e} - 2)(1-\varepsilon_2^2)$

$m_{23} = 0$

$m_{24} = 0$

$m_{25} = \mu_o R_2 (\ln 8R_2/r_{2e} - 2)(1-\varepsilon_5^2)$

$m_{26} = 0$

$m_{27} = 0$

$l_3 = \mu_o \pi^2 R_3/4k^2$; $k^2 = [4\alpha^2 1 + (1+8\alpha^2)^{1/2}][3 + (1+8\alpha^2)^{1/2}]^2/128\alpha^4$; $\alpha = -\varepsilon_3(n_v + 1/4)$;
$n_v = -(R/B_z) \cdot (\partial B_z/\partial R)$ = vertical field index at $R = R_1$

$m_{34} = \mu_o \pi R_4/2k \cdot \cos\delta_m \cdot (\varepsilon_{mz} - \varepsilon_{me})/\varepsilon_3$; $\varepsilon_{mz} = r_{mz}/R_4$; $\varepsilon_{me} = r_{me}/R_4$

$m_{35} = \mu_o \pi R_3/4k \cdot [\varepsilon_3((\ln 8R_3/r_3 - 1) + (r_5/r_3)^2 \varepsilon_3/2 - (R_3 - R_5)/r_3]$

$m_{36} = \mu_o \pi^2 R_3/4k \cdot (r_5/r_3)$

$m_{37} = \mu_o \pi^2 R_3/4k \cdot (r_5/r_3)^2 [3\varepsilon_3/4 + \alpha - (R_3 - R_5) r_5/r_3^2]$; $\alpha = -\varepsilon_3(n_v + 1/4)$; for n_v see l_3

$l_4 = \mu_o R_4 [(1+\varepsilon_{mz}\cos\delta_m) \cdot \ln[8R_4(1+\varepsilon_{mz}\cos\delta_m)((\varepsilon_{mz} - \varepsilon_{me})^2 + \varepsilon_{mz}\varepsilon_{me}(\Delta\delta_m)^2/r_{qz}(2 + (\varepsilon_{mz} + \varepsilon_{me})\cos\delta_m)^2]$
$+ 1/2 \cdot (1+\varepsilon_{me}\cos\delta_m) \cdot \ln[8R_4(1+\varepsilon_{me}\cos\delta_m)^2/r_{qz}\varepsilon_{me}\Delta\delta_m] + (0.2274\varepsilon_{mz} + 0.6932\varepsilon_{me})\cos\delta_m - 1{,}5312]$

$m_{45} = \mu_o R_4/2 \cdot (\varepsilon_{mz} - \varepsilon_{me})(\ln 8R5/r_{5e} - 1/2)\cos\delta_m$

$m_{46} = \mu_o \pi R_4/16 \cdot (\varepsilon_{mz} - \varepsilon_{me})/\varepsilon_5 \cdot [8\cos\delta_m + (\varepsilon_{mz} + \varepsilon_{me})(2 + 3\cos\delta_m)]$

$m_{47} = \mu_o \pi R_4/8 \cdot (\varepsilon_{mz} - \varepsilon_{me})/\varepsilon_5 \cdot [4(\varepsilon_{mz} + \varepsilon_{me})/\varepsilon_5 \cdot \cos 2\delta_m + (\varepsilon_{mz}^2 + \varepsilon_{mz}\varepsilon_{me} + \varepsilon_{me}^2 + 2\varepsilon_5^2)/\varepsilon_5 \cdot \cos\delta_m]$

$l_5 = \mu_o R_5 (\ln 8R_5/r_{5e} - 2)(1-\varepsilon_5^2)$

$m_{56} = \mu_o \pi R_5 \varepsilon_5/4 \cdot (\ln 8R_5/r_5 - 1/2)$

$m_{57} = 0$

$l_6 = \mu_o \pi^2 R_5/4$

$m_{67} = \mu_o 3\pi^2 R_5 \varepsilon_5/16$

(The angle denoted by θ_m in the text is denoted by δ_m throughout this table)

$l_7 = \mu_o \pi^2 R_5/2$

Table 1

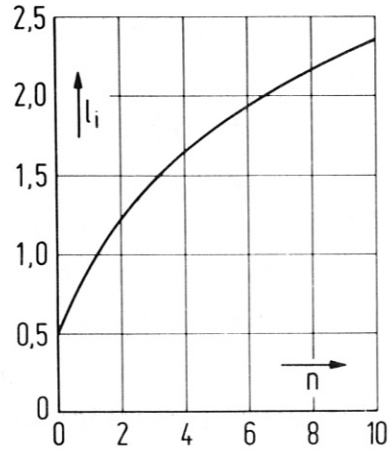

Fig. 6

to still more peaked j-profiles. Indeed, measurements of ℓ_i in PLT /8/ lead to $\ell_i \approx 2$, which according to Fig. 6 corresponds to $n \approx 6$, which in turn seems to be consistent with the T_e-profiles in PLT. Such high values have quite a strong bearing on the total plasma inductance L_1. The common practice of using $\ell_i = 0.5$ (i.e. $n = 0$), which corresponds to a flat current density profile, may therefore lead to L_1-values with a significant error.

4.2 Vertical field parameters ν_{a1}

Each coil current I_a produces a vertical magnetic field B_{a1} at the plasma centre $R = R_1$. This field is described by the vertical field parameters ν_{a1} introduced by eq. (18). The various ν_{a1} were calculated on the same basis as the inductances already described. The procedure is given in /2/ and /3/. No attempt was made to include corrections of more than the first order in ε_a or to include the effect of axial elongation e_a. The formulae for ν_{a1}/N_a are given in Table 2. The ν_{a1}/N_a are appropriate if ampere-turns are used instead of currents.

$$\nu_{21}/N_2 = 0$$

$$\nu_{31}/N_3 = \mu_o/4kr_3 \quad \text{(for k see } \ell_3 \text{ in Table 1)}$$

$$\nu_{41}/N_4 = \mu_o/2\pi r_{mz}.(r_{mz}/r_{me}-1)\cos\theta_m$$

$$\nu_{51} = \mu_o\varepsilon_5/4\pi r_5.(\ell n 8R_5/r_5-1/2)$$

$$\nu_{61} = \mu_o/4r_5$$

$$\nu_{71} = \mu_o\varepsilon_5/8r_5.[1 + (2/\varepsilon_5)^2.(R_1/R_5 -1)]$$

Table 2

4.3 Poloidal magnetic fields of the coil currents for arbitrary locations

Sometimes it is necessary to determine the poloidal fields not only at

the plasma centre but at some other location. This, in general, occurs if technical constraints in connection with magnetic fields have to be met. A well-known example is the so-called "core constraint", which leads to an upper limit of the admissible poloidal field produced at the transformer inner edge. For such general locations our assumption of weak toroidicity may easily be violated. For this case we therefore determine the magnetic field components B_z and B_R produced by toroidal line current distributions $i(\theta)$ or by filamentary current rings (magnetic limiter coils) at a point P(R,z) on the basis of Green's function of the Grad-Shafranow equation, which determines the flux functions of poloidal fields. Because this Green's function is known analytically (see p. 125 in /9/), it is possible to write the magnetic field components B_z and B_R at an arbitrary point P (see Fig. 7) in closed form.

We represent the line current density $i_a(\theta_s)$ in the following form:

$$i_a(\theta_s) = I_a/r_a.(f_o + f_1\cos\theta_s + f_2\cos 2\theta_s) \qquad (45)$$

(θ_s is the azimuth of the source point P_s on the curve $r = r_a$; I_a is the coil current; for details of its definition see /3/). The f_i follow from the desired poloidal fields inside the current-carrying shell, as described in /2/ and /3/. Besides geometric parameters the f_i contain the numbers of turns of the realistic coils, which are modelled by our current-carrying shells.

The geometry and the relevant geometric parameters are shown in Fig. 7.

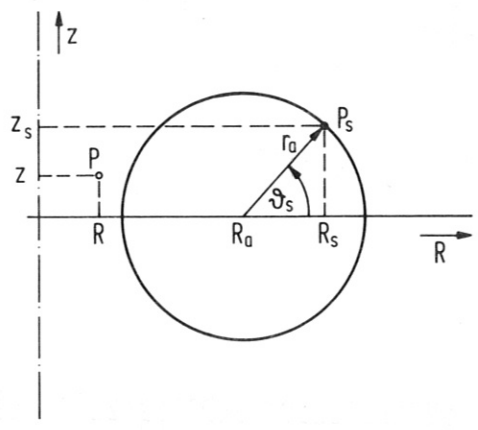

Fig. 7

The magnetic field components B_{az} and B_{aR} at P are related to the coil current I_a in the usual way:

$$B_{az} = \nu_{az}\, I_a, \qquad (46)$$

$$B_{aR} = \nu_{aR}\, I_a\,. \qquad (47)$$

For a distribution like (45) the functions ν_{az} and ν_{aR} are given by

$$\nu_{az} = \int_0^{2\pi} g_z(R,z;R_s,z_s) i_a(\theta_s) d\theta_s \ , \tag{48}$$

$$\nu_{aR} = \int_0^{2\pi} g_R(R,z;R_s,z_s) i_a(\theta_s) d\theta_s \ . \tag{49}$$

The kernels g_z and g_R of the integrals (48) and (49) follow from Green's function of the Grad-Shafranov equation:

$$g_z = \frac{\mu_0}{2\pi} \cdot \frac{1}{[(R+R_s)^2+(z-z_s)^2]^{1/2}} \cdot \left[K(k^2) + \frac{R_s^2+R^2-(z-z_s)^2}{(R-R_s)^2+(z-z_s)^2} E(k^2)\right] , \tag{50}$$

$$g_R = \frac{\mu_0}{2\pi} \cdot \frac{z-z_s}{R[(R+R_s)^2+(z-z_s)^2]^{1/2}} \cdot \left[-K(k^2) + \frac{R_s^2+R^2+(z-z_s)^2}{(R-R_s)^2+(z-z_s)^2} E(k^2)\right] , \tag{51}$$

$$\kappa^2 = \frac{4RR_s}{(R+R_s)^2+(z-z_s)^2} \ . \tag{52}$$

K and E are the complete elliptic integrals of the first and second kinds.

The functions ν_{az} and ν_{aR} also remain finite if P is located on the circle $r = r_a$. This is due to the fact that the $1/\rho$-singularity of g_z and g_R [$\rho^2 = (R-R_s)^2 + (z-z_s)^2$] which occurs for $P \longrightarrow P_s$ (i.e. $\kappa^2 \longrightarrow 1$), is compensated by the fact that the contribution from the current at $P = P_s$ is proportional to $d\theta_s$, which in turn is proportional to ρ. The product $1/\rho . d\theta_s$ leads to the discontinuity of the tangential magnetic field across a contour carrying a surface current normal to the field.

The integrals (48) and (49) can readily be evaluated numerically by using the polynomial approximations for K and E given in /10/.

If the current is not distributed according to eq. (45) but is a filamentary ring current I_a at $R = R_f$, $z = z_f$, we get for ν_{az} and ν_{aR}

$$\nu_{az} = g_z\,(R,z;R_f,z_f) \ , \tag{53}$$

$$\nu_{aR} = g_R\,(R,z;R_f,z_f) \ . \tag{54}$$

Equations (53) and (54) follow if we insert in eqs. (48) and (49) the δ-function which represents the filamentary current. It is obvious that for a filamentary current there remains a $1/\rho$-singularity for $R \rightarrow R_f$, $z \rightarrow z_f$. If the filamentary current ring has N_f turns, the factor N_f has to be added in front of eqs. (53) and (54).

4.4 Parameter F_{14} correlating plasma and magnetic limiter currents

For simplicity we assume that the current I_4 in the magnetic limiter coils at any instant is determined by the plasma current I_1. This assumption corresponds to a control of I_4 by I_1 with zero delay time.

Because of the multipole character we neglect the influence of the triples on each other for $N_{m\ell} = 2$, where $N_{m\ell}$ is the number of magnetic limiter coil triples. For $N_{m\ell}$ we allow the options 0 or 1 or 2.

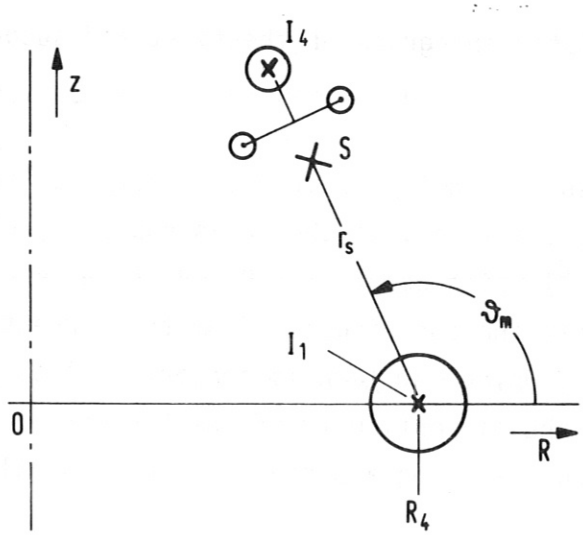

Fig. 8

For the case of a specified stagnation point S (see Fig. 8) the factor F_{14} correlating I_1 and I_4 can be derived by making some obvious simplifications as shown in /3/. The result is

$$F_{14} = N_4 I_4 / I_1 =$$

$$\frac{1-\tfrac{1}{2}\cdot(r_s/R_4)\left[r_s/r_s\cdot(\ln 8R_4/r_s - 2) - (r_s/r_s)\cdot(2_4 + \tfrac{1}{2})\right]\cos\theta_m}{r_s\,(1 + r_s/R_4\cdot\cos\theta_m)}$$

$$\times \frac{(r_{mz} - r_s)(r_{me}^2 + r_s^2 - 2 r_{me} r_s \cos\Delta\theta_m)}{r_{me}\,(r_{me} - r_s\cos\Delta\theta_m) + r_{me}\,(r_s - r_{me}\cos\Delta\theta_m)} \qquad (55)$$

(r_s = minor radius of stagnation point S; for r_{mz}, r_{me}, θ_m, and $\Delta\theta_m$ see Fig. 5).

4.5 Coil resistances

If we do not treat a concrete tokamak coil design where the various coils have known properties, we need formulae which allow of estimating the coil resistances R_{0a}.

For the resistance R_{01} of the plasma, which, in general, is a function of time, we shall not try to derive an analytical representation, but assume that R_{01} will always be given by a plasma model such as NUDIPLAS /11/ or by 1D models such as WHIST and BALDUR.

For R_{02}, R_{03}, and R_{04} (transformer primary, vertical field coils, magnetic limiter coils) we use the following procedure: we assume that one turn of a coil "a" will be designed for a nominal current I_{an}, and that technical constraints dictate an admissible gross current density j_g. For a conductor with the gross cross-section q_{ag} and filling factor α_f we get for the net conductor cross-section q_{an}

$$q_{an} = \alpha_f \, q_{ag} \, . \tag{56}$$

The resistance of one turn with major radius R_{ai} and net cross-section q_{an} is

$$R_{0ai} = 2\pi R_{ai}/(\sigma q_{an}) \, . \tag{57}$$

(σ = specific conductivity of the coil conductor).
q_{ag} can be expressed by I_{an} and j_g:

$$q_{ag} = I_{an}/j_g \, . \tag{58}$$

Equation (58) together with eqs. (56) and (57) leads to

$$R_{0ai} = 2\pi R_{ai} j_g/(\sigma \alpha_f I_{an}) \, . \tag{59}$$

By summing eq. (59) over all turns " i" of coil "a" we get the total coil resistance

$$R_{0a} = 2\pi j_g N_a \overline{R}_a/(\sigma \alpha_f I_{an}), \tag{60}$$

where $\overline{R_a}$ is an average turn radius given by

$$\overline{R_a} = 1/N_a . \sum_{i=1}^{N_a} R_{ai} \quad . \tag{61}$$

Finally, we introduce the nominal ampere-turns

$$A_{an} = N_a I_{an} \tag{62}$$

in eq. (60), which gives

$$R_{0a} = N_a^2 . 2\pi j_g \overline{R_a} / (\sigma \alpha_f A_{an}) . \tag{63}$$

We now specialize eq. (63) to transformer coils (a=2), vertical field coils (a=3), and magnetic limiter coils (a=4) by the following formulae:

$$\overline{R_2} = R_2 - r_2, \tag{64}$$

$$A_{2n} = I_{1n}/2m_{12} . [R_{01n}\, \tau_b (1+\tau_{1s}/\tau_b) + \ell_1], \tag{65}$$

$$\overline{R_3} = R_3, \tag{66}$$

$$A_{3n} = 1/2.4 |\nu_{1n}| k r_3 I_{1n}/\mu_o \ , \tag{67}$$

$$\overline{R_4} = R_4 \ (1 + \cos\theta_m) \ , \tag{68}$$

$$A_{4n} = 1/2 . F_{14} I_{1n} \tag{69}$$

(I_{1n} = nominal plasma current, τ_b = plasma current flow time, τ_{1s} = time necessary to establish the plasma current density profile, ν_{1n} = nominal value of ν_1).

R_2, R_3, and R_4 are estimates based on the following arguments:

- The bulk of the transformer primary windings is concentrated near the major torus axis, which leads to $\overline{R_2} \approx R_2 - r_2$.

- The windings of the vertical field coil are distributed nearly symmetrically with respect to $R = R_3$.

- The magnetic limiter coils are centred around the central coil at $R = R_4\ (1 + \cos\theta_m)$.

A_{2n} according to eq.(65) has been estimated by assuming a symmetrical transformer flux swing to cover the resistive and inductive flux consumptions. The time τ_{1s} accounts for the flux consumption during the establishment of the plasma current density profile /8/. A_{3n} is based on the vertical field current necessary for plasma equilibrium at nominal plasma parameters such as I_{1n}, R_{1n}, r_{1n} a.s.o. A_{4n} is based on the magnetic limiter current necessary for producing together with the nominal plasma current I_{1n} the stagnation point S (see Fig. 8). The factors 1/2 in eqs. (67) and (69) take into account that N_3 and N_4 are only half the turn numbers of the coils 3 and 4 (vertical field and magnetic limiter coils).

The resistances R_{05}, R_{06}, and R_{07} corresponding to the chamber current components I_5, I_6, and I_7 are determinated by the requirement that the dissipation produced by the corresponding line currents $i_a(\theta)$ introduced in Sec. 4.1 and $I_a^2 R_{0a}$ be identical. This leads to

$$I_a^2 R_a = \frac{2\pi R_5 r_5}{\sigma_c d_c} \int_0^{2\pi} j_a^2(\theta)(1 + \varepsilon_5 \cos\theta)\,d\theta,\ a = 5,\ 6,\ 7 \qquad (70)$$

(σ_c = electrical conductivity of chamber wall material, d_c = thickness of chamber wall). The $j_a(\theta)$ are given in /3/:

$$j_5(\theta) = I_5/2\pi r_5, \qquad (71)$$

$$j_6(\theta) = I_6/2r_5.\cos\theta, \qquad (72)$$

$$j_7(\theta) = I_7/r_5.\cos 2\theta. \qquad (73)$$

Formula (70) together with these $j_a(\theta)$ leads to

$$R_{05} = R_5/\sigma_c d_c r_c, \qquad (74)$$

$$R_{06} = \pi^2/2.R_{05}, \qquad (75)$$

$$R_{07} = 2\pi^2.R_{05}. \qquad (76)$$

These resistances lead to a correct determination of the dissipated energies. The ohmic voltage drops $I_a R_a$ are not correct, but this is of minor importance in the case of the plasma chamber.

5. Mathematical models of poloidal coil systems

We have used the material presented in the preceding sections to set up mathematical models for the pulsed coil systems of tokamaks. After computerization these models are used in the frame of the IPP systems studies.

The PCOILS 1 (Pulsed Coils 1) model is used for calculating the voltages, currents, powers and energies of tokamak coil systems without detailed allowance for plasma position control. The PCOILS 1 program forms part of our SISYFUS-TE tokamak power plant model. The basis of SISYFUS-TE is described in /12, 13/, its most recent improvements and extensions in /14/.

The PCOILS 2 model is intended for studying feedback position control of tokamak plasmas via the vertical magnetic field. Position control is both a subject of its own importance and a significant feature of controlling the lower ignition point of a tokamak plasma by compression / decompression schemes /15/. For studying such schemes PCOILS 2 will be coupled to the NUDIPLAS plasma model /11/.

5.1 The PCOILS 1 model

For systems studies it is important to have fast running computer programs. We therefore decided to set up a simple coil model which is capable of representing the main voltages, currents, and energies with reasonable accuracy and needs only short computing times.

The basic assumptions to achieve these goals are:

(a) The variations of the plasma dimensions (R_1,r_1) and the plasma

parameters (I_1, β_p, ℓ_i, e_1) with time are small on the time scales of toroidal and poloidal flux conservation.

(b) The delay time of the vertical field current adjustment to the variations listed above and to the fields of induced currents is negligible compared with the characteristic times of the above variations.

Assumption (a) means, for example, that PCOILS 1 cannot be used for studying adiabatic compression or fast compression / decompression control cycles. Because of assumption (a) it is possible to prescribe R_1, r_1, I_1, β_p, ℓ_i, and e_1 separately as functions of time without producing unphysically fast flux changes in the coil system. The fact that the parameters are independent of each other does not hold for fast changes can, for example, be seen for the case of I_1 and R_1, which are linked by the condition $d(I_1 R_1)/dt = 0$. This condition is contained in eqs. (29) and (31) because during fast but nonturbulent processes $dq/dt = 0$ is valid.

5.1.1 Equations

Given input as functions of time are:

(a) dI_1/dt time derivative of plasma current

(b) $d\beta_p/dt$ time derivative of poloidal beta

(c) $d\ell_i/dt$ time derivative of relative internal inductance

(d) de_1/dt time derivative of minor cross-section elongation

(e) dR_1/dt time derivative of major plasma radius

(f) dr_1/dt time derivative of minor plasma radius

(g) $R_{01}(t)$ plasma resistance

The derivatives (a) to (f) were chosen instead of the functions themselves for mathematical convenience in the coupling of PCOILS to plasma models. Obviously, the functions (a) to (f) have to be supplemented by the corresponding initial values at $t = t_0$:

$I_1(t_0)$, $\beta_p(t_0)$, $\ell_i(t_0)$, $e_1(t_0)$, $R_1(t_0)$, $r_1(t_0)$.

The dependent variables $I_2(t)$, $I_3(t)$, $I_4(t)$, $I_5(t)$, $I_6(t)$, and $I_7(t)$ are determined by

- the circuit equations (1), (5), (6), (7),

$$- (\nu_1 I_1)^{\cdot} = \sum_2^7 (\nu a_1 I_a)^{\cdot} . \tag{77}$$

$$- \dot{N}_4 I_4 = (F_{14} I_1)^{\cdot} . \tag{78}$$

Equation (77) expresses the instantaneous adjustment of the vertical field current I_3 to that value which is necessary to produce the equilibrium field $B_z = \nu_1 I_1$ [see eqs. (24) and (25)] if the contributions of I_2, I_3, I_4, I_5, I_6 according to eq. (19) are taken into account (assumption b from above).

Equation (78) is the differentiated form of eq. (55).

Equations (1), (5), (6), (7), (77), and (78) form a closed set of coupled differential equations to determine the currents $I_2(t)$ to $I_7(t)$ if the initial values of these currents are specified. We choose the following initial values:

$$\begin{aligned}
&I_2(t_0) \quad \text{given input to adjust flux swing,}\\
&I_3(t_0) = 1/\nu_{31}(t_0) \cdot [\nu_1(t_0) I_1(t_0) - \nu_{21}(t_0) I_2(t_0) - \nu_{41}(t_0) I_4(t_0)],\\
&I_4(t_0) = 1/N_4 . F_{14} I_1(t_0),\\
&I_5(t_0) = 0,\\
&I_6(t_0) = 0,\\
&I_7(t_0) = 0.
\end{aligned} \tag{79}$$

The currents $I_5(t_0)$, $I_6(t_0)$, $I_7(t_0)$ have been omitted from the equation for $I_3(t_0)$ because they were set equal to zero. This describes the assumption that chamber currents from a preceding tokamak cycle have already decayed.

5.1.2 Solution

Because the inductances, the resistances, and the parameters ν contain $N_a N_b$, N_a^2 or N_a as factors, it is possible to write all equations in terms of ampere-turns instead of currents. This eliminates the necessity of specifying the numbers of turns in the program input.

Equations (1), (5), (6), (77), and (78) can therefore be written as

$$\underline{\underline{B}}\ \dot{\underline{A}} = \underline{C} . \qquad (80)$$

$\underline{\underline{B}}$ is a 6 x 6 matrix whose elements are determined by the circuit parameters. In general, at least part of the matrix elements vary with time because of the varying plasma parameters. $\dot{\underline{A}}$ is the column vector formed by the time derivatives of the ampere-turns. The right-hand $\underline{C}$ is a column vector whose elements are made up by circuit parameters and the ampere-turns themselves.

For the numerical treatment $\underline{\underline{B}}$, $\underline{A}$, $\underline{C}$, and the time t are normalized to limit the orders of magnitude.

By matrix inversion eq. (80) leads to

$$\dot{\underline{\underline{A}}} = \underline{\underline{\underline{B}}}^{-1}\ \underline{C} . \qquad (81)$$

The system (81) of linear, ordinary differential equations is solved numerically. The calculation of $\underline{\underline{\underline{B}}}^{-1}$ has to be repeated for each time step when numerically integrating the system (81). This integration is done either by the Runge-Kutta method or by Hamming's modified predictor corrector method. Both methods are computerized as RKGS and HPCG respectively in the IBM "Scientific Subroutine Package".

If the plasma chamber has no slits in the poloidal direction, a mean current I_5 can develop and no slit voltage U_5 occurs ($U_5 \equiv 0$). If, on the other hand, at least one slit is present, the current I_5 is suppressed and eq. (5) has to be eliminated from our system of equations.

If the ampere-turns and hence also their derivatives are known the voltages per turn U_2/N_2 (transformer), U_3/N_3 (vertical field coil), and U_4/N_4 (magnetic limiter coils) are determinated from the circuit equations (2), (3), and (4). In the presence of a slit in the chamber, the voltage across the slit is calculated from eq. (5) taking into account $I_5 \equiv 0$.

On the basis of the ampere-turns and voltages per turn the powers according to eqs. (8) to (17) are calculated. The corresponding energies are determined by integration.

The magnetic fields at specified location, e.g. at the transformer inner edge, are calculated on the basis of the ampere-turns together with the ν_{az} and ν_{aR} determined numerically from eqs. (48) and (49).

5.1.3 Check of energy balance

To monitor the numerical accuracy, we check the overall energy balance at each time step. The energies involved are:

- energy E_e delivered to or extracted from the system via the the voltages U_2, U_3, and U_4,
- energy E_d dissipated by the various currents,
- energy E_f stored in the poloidal magnetic field,
- mechanical energy E_m due to varying geometrical plasma dimensions.

The associated energy differences between the times $t = t_0$ and arbitrary times $t \geq t_0$ are given by:

$$\Delta E_e = \sum_{a=2}^{4} \int_{t_0}^{t} U_a I_a dt, \qquad (82)$$

$$\Delta E_d = \sum_{a=1}^{7} \int_{t_0}^{t} I_a^2 R_a dt, \qquad (83)$$

$$\Delta E_f = \sum_{a=1}^{7} \frac{1}{2} [L_a(t) I_a^2(t) - L_a(t_0) I_a^2(t_0)] + \sum_{a=1}^{7} \sum_{a+1}^{7} [M_{ab}(t) I_a(t) I_b(t) - M_{ab}(t_0) I_b(t_0)], \quad (84)$$

$$\Delta E_m = \int_{t_0}^{t} \left(\sum_{a=2}^{7} I_1 I_a \dot{M}_{1a} + \frac{1}{2} I_1^2 \dot{L}_1 \right) dt. \quad (85)$$

Equation (85) takes into account that only the inductances involving the plasma (index "1") may vary with time. The various energy differences have to meet the balance

$$\Delta E_e = \Delta E_d + \Delta E_f + \Delta E_m . \quad (86)$$

We define an energy balance error ε_{eb} by

$$\varepsilon_{eb} = (\Delta E_e - \Delta E_d - \Delta E_f - \Delta E_m) / (|\Delta E_e| + |\Delta E_d| + |\Delta E_f| + |\Delta E_m|). \quad (87)$$

The error ε_{eb} is determined for each time step of the numerical integration and is monitored in the program output.

5.1.4 Stability problem due to severe idealizations

The idealizing assumption of instantaneous adjustment of the vertical field current I_3 made for PCOILS 1 in Sec. 5.1 may lead to solutions which diverge with time or, at least, produce numerical problems. The reason for that will be demonstrated in the following analysis.

We assume that the current I_5 is suppressed by a slit and restrict our analysis to terms of zero order in the ε's (inverse coil aspect ratios) on the left-hand sides of our equations (listed in Sec. 5.1.1). Furthermore, we neglect all variations of the plasma parameters with time except a variation of the plasma current I_1. We are thus left with the following two equations.

$$M_{36}\dot{I}_3 + L_6\dot{I}_6 + R_{06}I_6 = - M_{16}\dot{I}_1, \tag{88}$$

$$\nu_{31}I_3 + \nu_{61}I_6 = \nu_1 I_1. \tag{89}$$

Equation (89) expresses the instantaneous adjustment of the vertical field current I_3 to changes of I_1 (given from outside) and of the chamber dipole current I_6 (induced by $\dot{I}_1$ and $\dot{I}_3$).

Elimination of I_6 and $\dot{I}_6$ leads to

$$\tau\dot{I}_3 + I_3 = \nu_1/\nu_{31}\cdot(\tau_6 I_1 + \nu_3 M_{16}/\nu_1 R_6 \cdot \dot{I}_1 + I_1) \tag{90}$$

with

$$\tau = (L_6 - \nu_{61}M_{36}/\nu_{31})/R_{06}, \tag{91}$$

$$\tau_6 = L_6/R_{06}. \tag{92}$$

The character of the solutions of (90) depends on τ.
To demonstrate this we assume an $I_1(t)$ typical of the current start-up phase (see Fig. 9). For this $I_1(t)$ the right-hand side of eq. (90) jumps at t = 0 from zero to a finite value. For $\tau = 0$ a corresponding jump occurs in I_3. For $\tau > 0$ I_3 follows the jump of the r.h.s. delayed with the time constant τ; for $\tau < 0$, however, I_3 diverges exponentially with t. These cases are shown schematically in Fig. 9. In numerically solving our equations, already approaching $\tau = 0$ from the side $\tau > 0$ may cause numerical problems because of steep gradients with time. The fact that values $\tau \gtrsim 0$ or even $\tau < 0$ may occur can easily be shown by inserting L_6, M_{36}, ν_{31}, and ν_{61} from Tables 1 and 2 in eq. (81). The result

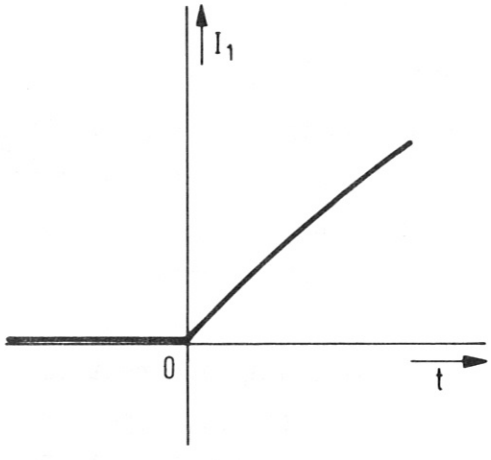

Fig. 9

$$\tau = \mu_0 \pi^2 / 4R_{06} \cdot (R_5 - R_3) \qquad (93)$$

shows that τ in our case will always be close to the margin $\tau = 0$ but with either positive or negative sign.

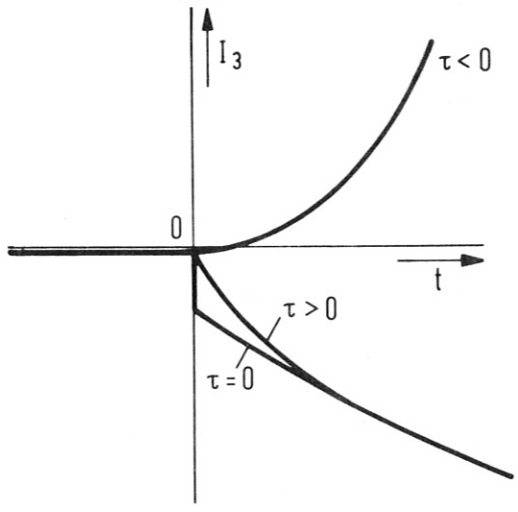

Fig. 10

Physically, the effects discussed above are due to the screening currents induced in the chamber walls via the mutual inductance M_{36}. $M_{36} = 0$ would lead to $\tau = L_6/R_{06}$ and thus always to a stable situation.

The program PCOILS 1 checks the value of ν_{31} and adjusts, if necessary, ν_{31} to 1.25 times the marginal value $\nu_{61}M_{36}/L_6$. Physically, this corresponds to the assumption that part of the field produced by I_3 directly leaks to the plasma centre through one or more poloidal slits. Without the check of ν_{31} the program PCOILS 1, in fact, produces solutions with very steep gradients or even divergence with time for $\nu_{31} \gtrsim \nu_{61}M_{36}/L_6$. The details depend on the higher-order contributions, which we have neglected in our analysis.

It is obvious that the difficulties described above are not physical ones but are induced by the strong simplifications adopted in PCOILS 1. In reality, the current I_3 will never adjust itself instantaneously so that in the case of a vertical field imbalance the plasma will shift. This shift produces changes in the mutual inductances of plasma and chamber components, thus inducing Foucault currents in the chamber walls. These currents stabilize the plasma position on the L/R-time scale of the chamber and thus allow of vertical field control with finite response time. These features will be treated in the frame of the coil model PCOILS 2.

5.2 The PCOILS 2 model

5.2.1 Equations

For the PCOILS 2 model we shall not assume that the major plasma radius R_1 and the plasma current I_1 can be prescribed separately. In reality, they are coupled during fast flux changes, as can be seen from eqs. (29) and (31).

As plasma parameters which may be controlled from outside or which may be considered as external disturbances we take into account:

the safety factor q,
the poloidal plasma beta (β_p),
the relative internal plasma inductance ℓ_i,
the plasma elongation e_1.

By analogy with PCOILS 1 we do not prescribe the above functions themselves but their time derivatives:

(a) dq/dt,
(b) $d\beta_p/dt$,
(c) $d\ell_i/dt$,
(d) de_1/dt

together with their initial values

$q(t_o)$,
$\beta_p(t_o)$,
$\ell_i(t_o)$,
$e_1(t_o)$.

Furthermore, we assume the following functions of time to be given:

$R_{01}(t)$ plasma resistance,
$\dot{R}_n(t)$ time derivative of the nominal value of the major plasma radius, which is the reference input to be compared with the output function $R_1(t)$.

The necessary equations have already been collected in Sec. 3. From this set we use:

- the circuit equations (1), (3), (5), (6), (7),
- the relation $N_4\dot{I}_4 = (F_{14}I_1)^{\cdot}$ derived from (55),
- eq. (26), which determines R_1,
- eq. (29), giving the relation between R_1 and r_1,
- eq. (31), giving the relation between I_1, R_1, and r_1,
- eq. (19), giving the various contributions to B_z.

These 10 equations are coupled with each other. This is mainly due to the dependence of all inductances involving the plasma on the major plasma radius R_1 and in some cases also on the minor plasma radius r_1 and other plasma parameters.

We have a total of 15 differential equations for the 15 variables:

$$q,\ \beta_p,\ \ell_i,\ e_1,\ R_n,\ I_1,\ I_2,\ I_3,\ I_4,\ I_5,\ I_6,\ I_7,\ R_1,\ r_1,\ B_z.$$

The voltage U_3 occurring in eq. (3) consists of two components: U_{3ff} and U_{3fb}.

U_{3ff} is a feedforward voltage which is determined by the input variables ($\dot{q}$, $\dot{\beta}_p$, $\dot{\ell}_i$, $\dot{e}_1$, $\dot{R}_n$). It is only possible to fix the mathematical form of U_{3ff} if the special problem to be treated is defined.

U_{3fb} is a feedback voltage which is given by

$$U_{3fb} = -U_{3n}/R_{10} \cdot G \left[\tau_d (R_n - R_1)^{\cdot} + (R_n - R_1) + 1/\tau_i \int_{t_o}^{t} (R_n - R_1)\,dt\right] \qquad (94)$$

(R_{10} = normalization value of the major plasma radius R_1).

Equation (94) describes a feedback control with gain G of the major plasma radius R_1 consisting of three components:

- a differential contribution with caracteristic time τ_d (first term),

- a proportional contribution (second term),
- an integral contribution with characteristic time τ_i (third term).

U_{3n} is a normalization value which may be chosen according to practical considerations. The negative sign preceding the r.h.s. of eq. (94) occurs because $\nu_1 < 0$ for the current directions we have chosen (see Fig. 1).

The feedback system is shown schematically in Fig. 11. This figure shows

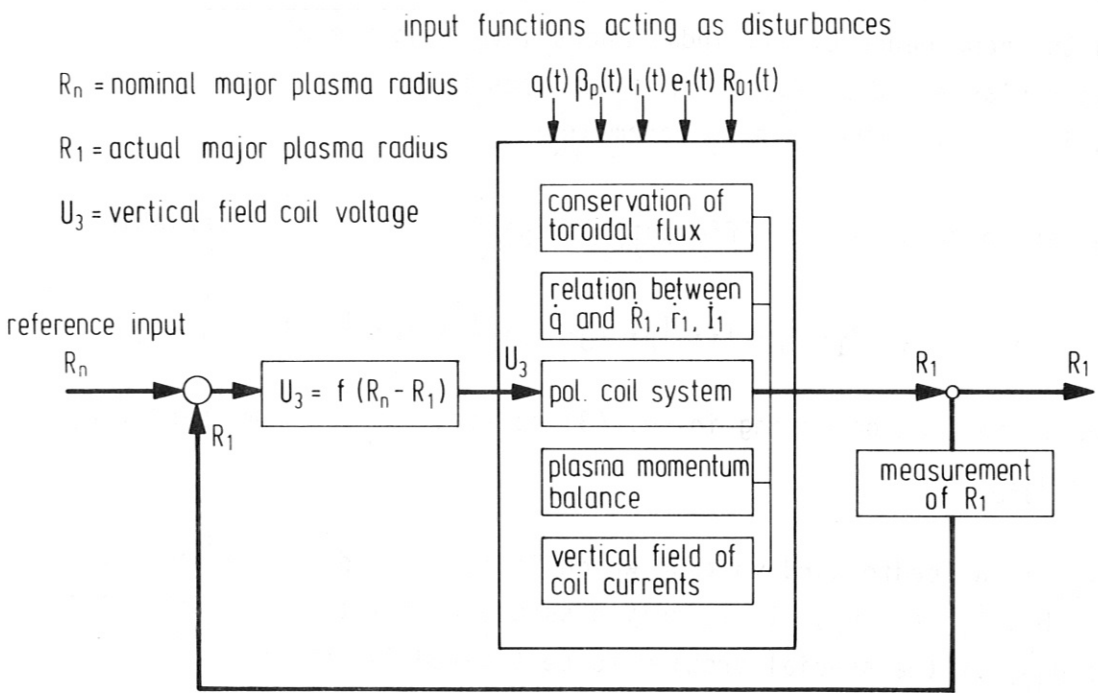

Fig. 11

that the functions

$$R_n(t),\ q(t),\ \beta_p(t),\ \ell_i(t),\ e_1(t),\ R_{01}(t)$$

act as input to the system, which itself is characterized by a set of 10 coupled differential equations which determine the state variables of the system:

$$I_1(t),\ I_2(t),\ I_3(t),\ I_4(t),\ I_5(t),\ I_6(t)\ I_7(t),\ R_1(t),\ r_1(t),\ B_z(t).$$

The output variable of the system is the major plasma radius $R_1(t)$.

In matrix notation our system reads

$$\underline{\underline{B}}\ \dot{\underline{Y}} = \underline{\underline{C}}\ \underline{Y} + \underline{\underline{D}}\ \underline{I}\ , \tag{95}$$

where $\underline{Y}$ is the vector of the state variables and $\underline{I}$ the vector of the input variables.

Matrix inversion transforms the system (95) into

$$\dot{\underline{Y}} = \underline{\underline{S}}\ \underline{Y} + \underline{\underline{G}}\ \underline{I}\ . \tag{96}$$

$\underline{\underline{S}}$ is the state matrix of the system, $\underline{\underline{G}}$ is the disturbance matrix representing the influence of the input variables. In our case $\underline{\underline{S}}$ is a 10 x 10 matrix and $\underline{\underline{G}}$ is a 10 x 6 matrix. The matrix $\underline{\underline{S}}$ governs the internal dynamics of our system, especially its stability. At least part of the elements of $\underline{\underline{S}}$ and $\underline{\underline{G}}$ in our case vary with time.

5.2.2 Solution

The solution of the system (95) for $\dot{\underline{Y}}$ is done numerically within the PCOILS 2 program. The resulting system of ordinary differential equations is solved numerically as in the case of PCOILS 1 (see Sec. 5.1.2).

As initial conditions we prescribe:

$$I_1(t_o) = 2\pi B_t(R_1)R_1/\mu_o \cdot [r_1 / R_1(t_0)]^2 \cdot 1/q(t_o)\ , \tag{97}$$

$I_2(t_o)$ prescribed so that it meets flux swing requirements,

$$I_3(t_o) = \begin{cases} 0 \quad \text{if} \quad I_1(t_o) = 0 & (98) \\ 1/\nu_{31}\cdot[\nu_1(t_o)I_1(t_o) - \nu_{21}I_2(t_o) - \nu_{41}I_4(t_o)], & (99) \end{cases}$$

$$I_4(t_o) = 1/N_4 \cdot F_{14}(t_o)I_1(t_o), \tag{100}$$

$$I_5(t_o) = 0\ , \tag{101}$$

$$I_6(t_o) = 0\ , \tag{102}$$

$$I_7(t_o) = 0 \ , \tag{103}$$

$$R_1(t_o) = \begin{cases} R_5 \left[1+1/2.(r_5/R_5)^2 \left[\ell n(r_5/r_1(t_o)+(1-r_1^2(t_o)/r_5^2) \right.\right. \\ \qquad \left.\left. *(\lambda_1(t_o)+1/2)\right]\right], \text{ if } I_1(t_o) = 0 \\ \text{prescribed at will if } I_1(t_o) \neq 0 \ , \end{cases} \tag{104}$$

$r_1(t_o)$ prescribed in accordance with start-up scenario chosen,

$$B_z(t_o) = \begin{cases} 0 \quad \text{if} \quad I_1(t_o) = 0 & (105) \\ \nu_1(t_o) I_1(t_0) \ . & (106) \end{cases}$$

$I_1(t_o)$ according to eq. (97) is the plasma current which corresponds to the starting value $q(t_o)$ of the safety factor at the plasma edge. Only very large values for $q(t_o)$ result in $I_1(t_o) = 0$ in the numerical sense of a computer program.

$I_2(t_o)$ is chosen in accordance with flux swing requirements such as a symmetrical swing over the total plasma current flow time τ_b. Mathematically, there are no limitations imposed on $I_2(t_o)$.

$I_3(t_o)$ according to eq. (98) would correspond to the limiting case $q(t_o) \longrightarrow \infty$. Underlying eq. (99) is the assumption that for $t = t_o$ the plasma has the equilibrium position $R_1(t_o)$ for the starting values of all relevant plasma parameters (r_1, β_p, ℓ_i, e_1) under the combined action of the coil currents $I_2(t_o)$, $I_3(t_o)$, and $I_4(t_o)$. Already taken into account are the zero initial values of the chamber currents I_5, I_6, and I_7.

$I_4(t_o)$ according to eq. (100) is fixed by $I_1(t_o)$ and by the position of the stagnation point as expressed by the function F_4 given by eq. (55).

$I_5(t_o)$, $I_6(t_o)$, $I_7(t_o) = 0$ describe the assumption that the chamber currents from a previous discharge have already decayed.

$R_1(t_o)$ according to eq. (104) is the equilibrium major radius determined by the interaction of the plasma current with the chamber dipole current I_6 induced via the mutual inductance M_{16}, which itself depends on R_1 (see Sec. 5.2.3). We adopt this $R_1(t_o)$ if $I_1(t_o)$ is zero. If $I_1(t_o)$ is not zero, which occurs if, for example, a previous calculation is continued, one has to choose $R_1(t_o)$ in keeping with this situation.

The minor plasma radius $r_1(t_o)$ has to be chosen in accordance with the start-up scenario adopted or with the calculation to be continued.

$B_z(t_o)$ according to eq. (105) corresponds to a zero initial plasma current $I_1(t_o)$ because of eq. (24). If $I_1(t_o) \neq 0$, we assume by eq. (106) that B_z has the value necessary for establishing the equilibrium position $R_1(t_o)$ chosen. This value of B_z is produced by $I_3(t_o)$ according to eq. (99).

As in the case of PCOILS 1, the PCOILS 2 program actually uses ampere-turns instead of currents and is written in terms of normalized variables.

The calculation of voltages, powers, energies, and magnetic field components proceeds as described in Sec. 5.1.2. The energy balance is checked by the procedure described in Sec. 5.1.3.

5.2.3 Equilibrium on the chamber current time scale

Because the mutual inductances between plasma and chamber components depend on the major plasma radius R_1, a moving plasma induces currents in the chamber walls. They produce B_z-components which impede the plasma motion and thus lead to a stabilization of plasma position for a limited time. This phenomenon is important if fast changes of the plasma parameters occur. Slow variations can be handled by feedback control via the vertical field coil current.

The fundamentals of wall stabilization by chamber currents can easily be investigated by using our formulae for inductances and magnetic field parameters. In the following we restrict ourselves to the action of the chamber dipole current I_6, By neglecting the influence of all currents except I_1 (plasma current) and I_6 we get from eq. (1) on the inductive time scale:

$$(M_{16}I_1)^{\cdot} + L_6 \dot{I}_6 = 0 \text{ for } (t-t_o) \ll L_6/R_{06} \qquad (107)$$

(t_o = initial value of t).

Assuming for the moment the initial condition

$$I_1(t_o) = 0$$

we get

$$I_6 = -M_{16}/L_6 . I_1 , \tag{108}$$

which leads to

$$B_z = - \nu_{61} M_{16}/L_6 . I_1 . \tag{109}$$

This field inserted in eq. (23) leads to an implicit equation for R_1. Important is the fact that R_1 is contained in M_{16}. Variations of R_1 thus lead to variations of I_6 even for constant I_1. By solving the implicit equation for R_1 we get the equilibrium position of the plasma column on the inductive time scale. The result, including terms up to order ε^2, is

$$R_1/R_5 = 1 + 0.5\ (r_5/R_5)^2 [\ell n\ r_5/r_1 + (1-r_1^2/r_5^2)\ (\lambda_1 + 1/2)]. \tag{110}$$

This is the well-known formula given in /1/.

We now assume that an extra magnetic field B_e is present which leads to

$$B_z = -\nu_{61} M_{16}/L_6 . I_1 + B_e . \tag{111}$$

We assume that the change of R_1 produced by B_e is of the same order as the shift by I_6 alone. The same procedure as above leads to the equilibrium radius

$$R_1/R_5 = 1 + 0.5\ (r_5/R_5)^2 [\ell n r_5/r_1 + (1-r_1^2/r_5^2)\ (\lambda_1+1/2)] + 2\pi/\mu_o . r_5^2/R_5 . B_e/I_1 . \tag{112}$$

If we now assume that $I_1(t_o) \neq 0$, and that the column with this current has the initial equilibrim position $R_1 = R_1(t_o)$, we get

$$B_e = \nu_{61} M_{16}(t_o)/L_6 . I_1(t_o) + \nu_1(t_o) I_1(t_o) . \tag{113}$$

The first term in eq. (113) stems from the initial condition for I_1 in the integration of (107), the second is the necessary equilibrium field for $t = t_o$ according to (24) and (25).

Insertion of (113) in (112) and calculation up to order ε^2 leads to

$$R_1/R_5 = 1 + 0.5\,(r_5/R_5)^2[\ell n r_5/r_1 + (1-r_1^2/r_5^2)\,(\lambda_1 + 1/2)]$$
$$- 0.5\,I_1(t_o)/I_o(r_5/R_5)^2[\ell n r_5/r_1(t_o) + (1-r_1^2(t_o)/r_5^2)\,(\lambda_1(t_o) + 1/2)]$$
$$+ I_1(t_o)/I_1 \cdot [R_1(t_o) - R_5]/R_5. \qquad (114)$$

Equation (114) describes the trajectory of R_1 on the inductive time scale if one starts from the equilibrium position $R_1 = R_1(t_o)$.

The equilibrium position (110) for $I_1(t_o) = 0$ has been used as initial condition (104) in Sec. 5.2.2.

The coupling constant $k_{36} = M_{36}/(L_3L_6)^{1/2}$ between the vertical field coil and the dipole contribution of the plasma chamber has been omitted up to now in spite of the fact that it is rather large (typically $k_{36} \approx 0.7$ to 0.9). In reality this close coupling leads to an inductive time scale τ_c of the chamber, which approximately is given by $(1 - k_{36}^2) \cdot L_6/R_6$. This time scale is much shorter than L_6/R_6 the value pertaining to the case without coupling. For times larger than τ_c the vertical field coils act stabilizing instead of the chamber. This stabilization is operational for times of the order $\tau_3 = L_3/R_3$. The equilibrium position R_1 of the plasma for this case can be found from (112) or (114) by using R_3, r_3 instead of R_5, r_5.

6. Sample calculations

6.1 Calculations for the ASDEX divertor tokamak

We have used PCOILS 1 and PCOILS 2 to model the operation of the ASDEX divertor tokamak.

The data used for PCOILS 1 is shown in Table 3, which is a reproduction of the program input listing. The starting value $R_1(0) = 1.71$ m was calculated from eq. (110).

```
PCOILS1 INPUT PARAMETERS :
**************************

NUMBER OF TIME POINTS TO BE CALCULATED                          NT     =          312 (-)
NUMBER OF TIME POINTS FOR PRESCRIBED FUNCTION                   NTF    =          121 (-)

ISLIT : 0 / 1 -> NO POLOIDAL / POLOIDAL SLIT                    ISLIT  =            1
IYOUT : 0 / 1 -> NO OUTPUT / OUTPUT OF Y(T,I)  I=1,26           IYOUT  =            1
IBOUT : 0 / 1 -> NO OUTPUT / OUTPUT OF BZ(GR=GRTI,Z=0)          IBOUT  =            1
IPOUT : 0 / 1 -> NO OUTPUT / OUTPUT OF POWERS                   IPOUT  =            1
IEOUT : 0 / 1 -> NO OUTPUT / OUTPUT OF ENERGIES                 IEOUT  =            1
IAOUT : 0 / 1 -> NO OUTPUT / OUTPUT OF AMPERETURNS AND
                             VOLTAGES PER TURN                  IAOUT  =            1
IFOUT : 0 / 1 -> NO OUTPUT / OUTPUT OF FUNCTIONS
                             CALCULATED FROM INPUT              IFOUT  =            1
JINT : RKGS / HPCG -> INTEGRATION BY
                RUNGE KUTTA / PREDICTOR CORRECTOR               JINT   =    RKGS
ITAB : 0 / 1 -> INPUT FUNCTIONS CALCULATED FROM GIVEN
FORMULAE/ INPUT FUNCTIONS CALCULATED FROM TABULATED INPUT       ITAB   =            0

START TIME FOR THE CALCULATION                                  TO     =    0.0          (S)
TIME STEP FOR THE OUTPUT                                        DT     =    4.00000E-04  (S)
TIME STEP OF INTEGRATION ROUTINE                                DTR    =    1.00000E-04  (S)

NORMALIZATION TIME CHARACTERISTIC OF CURRENT CHANGES            TAUN   =    5.00000E-02  (S)
PLASMA CURRENT FLOW TIME                                        TAUB   =    1.20000E+00  (S)
TOTAL CYCLE TIME                                                TAUC   =    1.20000E+00  (S)

CURRENT RAMP UP TIME                                            TAURU  =    4.00000E-02  (S)
CURRENT RAMP DOWN TIME                                          TAURD  =    4.00000E-02  (S)
BETA RAMP UP TIME                                               TAUBT  =    1.00000E+10  (S)

ACCURACY LIMIT OF NUMERICAL INTEGRATION PROCEDURE               EPSN   =    1.00000E-04  (-)

MAJOR RADIUS OF TRANSFORMER COIL CENTRE                         GRTR   =    1.69000E+00  (M)
MAJOR RADIUS OF VERTICAL FIELD COIL CENTRE                      GRV    =    1.73000E+00  (M)
MAJOR RADIUS OF CENTRAL MAGNETIC LIMITER COIL CENTRE            GRMZ   =    1.65000E+00  (M)
MAJOR RADIUS OF CHAMBER CENTRE                                  GRC    =    1.65000E+00  (M)
MAJOR RADIUS OF TRANSFORMER INNER EDGE                          GRTI   =    8.75000E-01  (M)

MINOR RADIUS OF TRANSFORMER COIL                                RTR    =    7.85000E-01  (M)
MINOR RADIUS OF VERTICAL FIELD COIL                             RV     =    7.25000E-01  (M)
DISTANCE OF CENTRAL MAGNETIC LIMITER COIL FROM CENTRE           RMZ    =    6.85000E-01  (M)
DISTANCE OF EXCENTRIC MAGNETIC LIMITER COIL FROM CENTRE         RME    =    5.60000E-01  (M)
MINOR CHAMBER RADIUS                                            RC     =    6.30000E-01  (M)
PLASMA CENTRE SEPARATRIX DISTANCE                               RS     =    4.70000E-01  (M)

MINOR Z-HALF HEIGHT OF TRANSFORMER COIL                         ZTR    =    1.40000E+00  (M)
MINOR Z-HALF HEIGHT OF VERTICAL FIELD COIL                      ZV     =    1.22000E+00  (M)
MINOR Z-HALF HEIGHT OF CHAMBER                                  ZC     =    1.17000E+00  (M)

THICKNESS OF CHAMBER WALL                                       DC     =    2.65000E-03  (M)
CROSS SECTIONAL RADIUS OF CENTRAL MAGNETIC LIMITER COIL         RQZ    =    6.35000E-02  (M)

ANGLE BETWEEN R-AXIS AND RMZ                                    TETAM  =    1.00000E+02  (DEGREE)
ANGLE BETWEEN RMZ AND RME                                       DTETAM=     2.00000E+01  (DEGREE)

NUMBER OF TURNS , TRANSFORMER COIL                              GNTR   =    1.00000E+02  (-)
NUMBER OF TURNS IN ONE CURRENT DIRECTION  , VERT. F. COIL       GNV    =    8.00000E+00  (-)
NUMBER OF TURNS , CENTRAL MAGNETIC LIMITER COIL                 GNMZ   =    8.00000E+00  (-)

NUMBER OF MAGNETIC LIMITER COIL TRIPLES (0,1,2 OPTIONAL)        NML    =    2.00000E+00  (-)

ELECTRICAL CONDUCTIVITY OF CHAMBER MATERIAL                     SIGC   =    9.50000E+05  (1/(OHM*M))
VERTICAL FIELD INDEX                                            NV     =    1.00000E+00  (-)

RESISTANCE OF TRANSFORMER COIL                                  GRT    =    1.27000E-02  (OHM)
RESISTANCE OF VERTICAL FIELD COIL                               GRVV   =    2.25000E-03  (OHM)
RESISTANCE OF ONE SET OF LIMITER COILS                          GRML   =    1.33000E-03  (OHM)

STARTING VALUE OF TRANSFORMER CURRENT                           ITRTO  =    2.70000E+04  (A)
STARTING VALUE OF CHAMBER CURRENT IC0                           ICOTO  =    0.0          (A)
STARTING VALUE OF CHAMBER CURRENT IC1                           IC1TO  =    0.0          (A)
STARTING VALUE OF CHAMBER CURRENT IC2                           IC2TO  =    0.0          (A)
STARTING VALUE OF PLASMA CURRENT                                IPLTO  =    5.00000E+02  (A)
STARTING VALUE OF MINOR PLASMA RADIUS                           RPLTO  =    4.00000E-01  (A)
STARTING VALUE OF MAJOR PLASMA RADIUS                           GRPLTO=     1.65000E+00  (A)
STARTING VALUE OF REL. INT. PLASMA INDUCTANCE                   LITO   =    1.14000E+00  (-)
STARTING VALUE OF POLOIDAL PLASMA BETA                          BTPTO  =    1.87500E-03  (-)
STARTING VALUE OF PLASMA ELONGATION RATIO                       EPLTO  =    1.00000E+00  (-)

NORMALIZATION VALUE OF PLASMA CURRENT (FLAT TOP VALUE)          IPLO   =    5.00000E+05  (A)
NORMALIZATION VALUE OF MAJOR PLASMA RADIUS (NOMINAL VALUE)      GRPLO  =    1.65000E+00  (M)
NORMALIZATION VALUE OF MINOR PLASMA RADIUS (NOMINAL VALUE)      RPLO   =    4.00000E-01  (M)
NORMALIZATION VALUE OF PLASMA RESISTANCE                        GRPO   =    1.00000E-06  (OHM)
NORMALIZATION VALUE OF POL. PLASMA BETA (FLAT TOP VALUE)        BETAPO=     6.50000E-01  (-)
NORMALIZATION VALUE OF REL. INT. PLASMA INDUCTANCE              LIO    =    1.00000E+00  (-)
NORMALIZATION VALUE OF PLASMA ELONGATION                        EPLO   =    1.00000E+00  (-)
```

Table 3

The input functions

$$\dot{I}_1(t),\ \dot{\beta}_p(t),\ \dot{\ell}_i(t),\ \dot{e}_1(t),\ \dot{R}_1(t),\ \dot{r}_1(t),\ \dot{R}_{01}(t)$$

were specified as follows:

$$\dot{I}_1(t) = 4I_{10}/\tau_{ru} \cdot \exp(-4t/\tau_{ru}) \tag{115}$$

$$\begin{aligned} &\dot{\beta}_p(t) = 3.2036 \quad \text{for} \quad t < 0.04\ \text{s} \\ &\dot{\beta}_p(t) = 0 \quad \text{for} \quad 4.10^{-2}\ \text{s} < t \leq 0.1\ \text{s} \\ &\dot{\beta}_p(t) = 2.600 \quad \text{for} \quad 0.1\ \text{s} \leq t < 0.3\ \text{s} \\ &\dot{\beta}_p(t) = 0 \quad \text{for} \quad t \leq 0.3\ \text{s} \end{aligned} \tag{116}$$

$$\dot{\ell}_i(t) = 0 \tag{117}$$

$$\dot{e}_1(t) = 0 \tag{118}$$

$$\dot{R}_1(t) = 0 \tag{119}$$

$$\dot{r}_1(t) = 0 \tag{120}$$

$$\begin{aligned} &R_{01}(t) \sim 1/I_1(t) \quad \text{for } t < 0.1\ \text{s} \\ &R_{01}(t) = 4\text{x}10^{-7}\ \Omega \quad \text{for } t \leq 0.1\ \text{s}\ . \end{aligned} \tag{121}$$

The initial values necessary for evaluating eqs. (115) to (121) are

$$I_1(0) = 5 \times 10^2\ \text{A}$$

$$\beta_p(0) = 1.857 \times 10^{-3}$$

$$\ell_i(0) = 1.14$$

$$e_1(0) = 1$$

$$R_1(0) = 1.65\ \text{m}$$

$$r_1(0) = 0.40\ \text{m}$$

$$R_{01}(0) = 1.584\text{x}10^{-3}\ \Omega.$$

For the flat top plasma current I_{10} and for the current ramp up time τ_{ru} appearing in eq. (115) we use

$$I_{10} = 5 \times 10^5\ \text{A},\ \tau_{ru} = 4 \times 10^{-2}\ \text{s}.$$

The ramp up of β_p for $t < 0.04$ s models the increase of β_p due to ohmic heating and the ramp up for $t \geq 0.1$ s models

the effect of neutral beam injection starting at t = 0.1 s with a pulse duration of 0.2 s.

The relationship $R_{01} \sim 1/I_1$ roughly models the increase of plasma electrical conductivity due to ohmic heating. For $t \geq 0.1$ s (beam heating phase) we assume a small, constant value of R_{01} (roughly corresponding to $T_e(0) = 2.5$ keV). The impact of this choice on currents and voltages is very small.

The starting value $I_1(0) = 5 \times 10^2$ A was chosen to allow comparison with results from PCOILS 2, where $I_1(0) = 0$ is not allowed because of $q \sim 1/I_1$. The values $\beta_p(0)$ and $R_{01}(0)$ are estimates based on $n(r=0) \approx 10^{14}$ cm^{-3}, $T_e(r=0) \approx 10$ eV and approximately parabolic profiles $n(r)$, $T_e(r)$.

The value of $\ell_i(0)$ follows from Fig. 6 for n = 1.715. This value together with the current density profile (44) and $q(r=0) = 1$ leads to $q(r_1) = 2.715$, which is the value following from the nominal values $I_1 = 5 \times 10^5$ A, $R_1 = 1.65$ m, $r_1 = 0.40$ m envisaged for ASDEX.

The inductances, magnetic field parameters, and resistances calculated from the input data are as follows (MKSA-units):

$\ell_1 = 3.8964 \times 10^{-6}$
$m_{12} = 1.0202 \times 10^{-6}$
$m_{13} = 8.1370 \times 10^{-7}$
$m_{14} = -4.0270 \times 10^{-7}$
$m_{15} = 1.2978 \times 10^{-6}$
$m_{16} = 1.2403 \times 10^{-6}$
$m_{17} = 1.2978 \times 10^{-6}$

$\ell_2 = 9.2764 \times 10^{-7}$
$m_{23} = 0$
$m_{24} = 0$
$m_{25} = 4.6382 \times 10^{-7}$
$m_{26} = 0$
$m_{27} = 0$

$\ell_3 = 4.3604 \times 10^{-6}$
$m_{34} = -9.2179 \times 10^{-8}$
$m_{35} = 1.3312 \times 10^{-6}$
$m_{36} = 4.2026 \times 10^{-6}$
$m_{37} = 1.2989 \times 10^{-6}$

$\ell_4 = 4.3281 \times 10^{-6}$
$m_{45} = -3.0450 \times 10^{-8}$
$m_{46} = -2.2065 \times 10^{-8}$
$m_{47} = -1.2529 \times 10^{-6}$

$\ell_5 = 1.2978 \times 10^{-6}$
$m_{56} = 1.3883 \times 10^{-6}$
$m_{57} = 0$

$\ell_6 = 5.1160 \times 10^{-6}$
$m_{67} = 1.4650 \times 10^{-6}$

$\ell_7 = 1.0232 \times 10^{-5}$
$\nu_1 = -1.9070 \times 10^{-7}$
$\nu_{21}/N_2 = 0$
$\nu_{31}/N_3 = 3.1255 \times 10^{-6}$
$\nu_{41}/N_4 = -1.8107 \times 10^{-7}$
$\nu_{51} = 1.5408 \times 10^{-7}$
$\nu_{61} = 4.9867 \times 10^{-7}$
$\nu_{71} = 9.5110 \times 10^{-8}$

$R_{05} = 1.0403 \times 10^{-4}$
$R_{06} = 5.1339 \times 10^{-4}$
$R_{07} = 2.0535 \times 10^{-3}$

L/R times calculated from these values, from the normalization value $R_{010} = 10^{-6}\ \Omega$ of the plasma resistance, and from the given R_{02}, R_{03}, R_{04} are:

$L_1/R_{010} = 3.8964$ s
$L_2/R_{02} = 7.3042 \times 10^{-1}$ s
$L_3/R_{03} = 1.2403 \times 10^{-1}$ s
$L_4/R_{L4} = 2.0827 \times 10^{-1}$ s
$L_5/R_{05} = 1.2475 \times 10^{-2}$ s
$L_6/R_{06} = 9.9653 \times 10^{-3}$ s
$L_7/R_{07} = 4.9826 \times 10^{-3}$ s .

Whenever it was necessary in the calculation of the preceding values to specify R_1, r_1, β_p, ℓ_i, and e_1 we used the normalization values given in Table 3. The calculated values therefore approximately reflect the numbers we deal with but not in every case, the precise value occurring in the circuit calculation.

Figure 12 shows the various currents and voltages as functions of time during the first 125 ms of operation. Because the existence of a poloidal slit for suppressing the chamber current I_5 was assumed, a voltage U_5 develops across that slit. The maximum value U_{5max} = 48.2 V occurs at t = 0.

The input data for the corresponding calculation with PCOILS 2 is listed in Table 4.

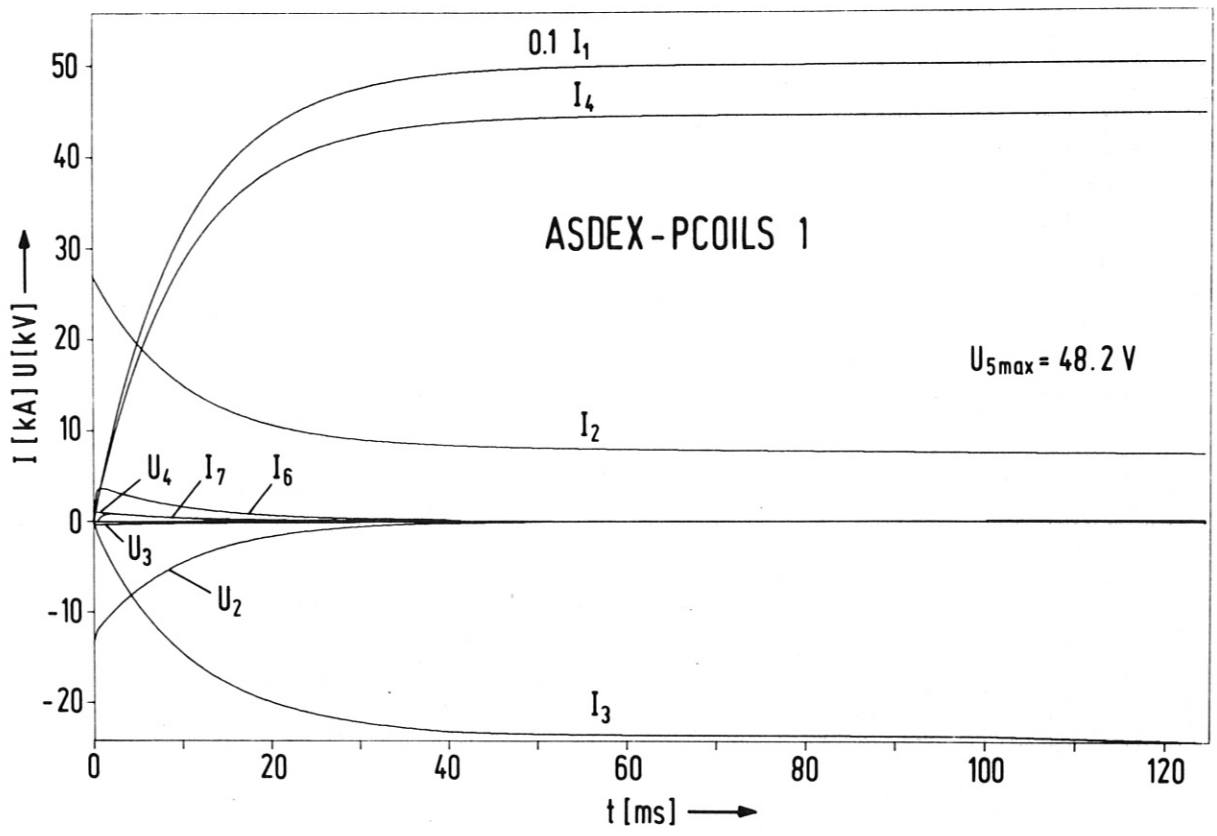
0.1 I1
I4
ASDEX-PCOILS 1
U5max = 48.2 V
I2
U4
I7
I6
U3
U2
I3
I [kA] U [kV]
t [ms]
50
40
30
20
10
0
-10
-20
0
20
40
60
80
100
120

Fig. 12

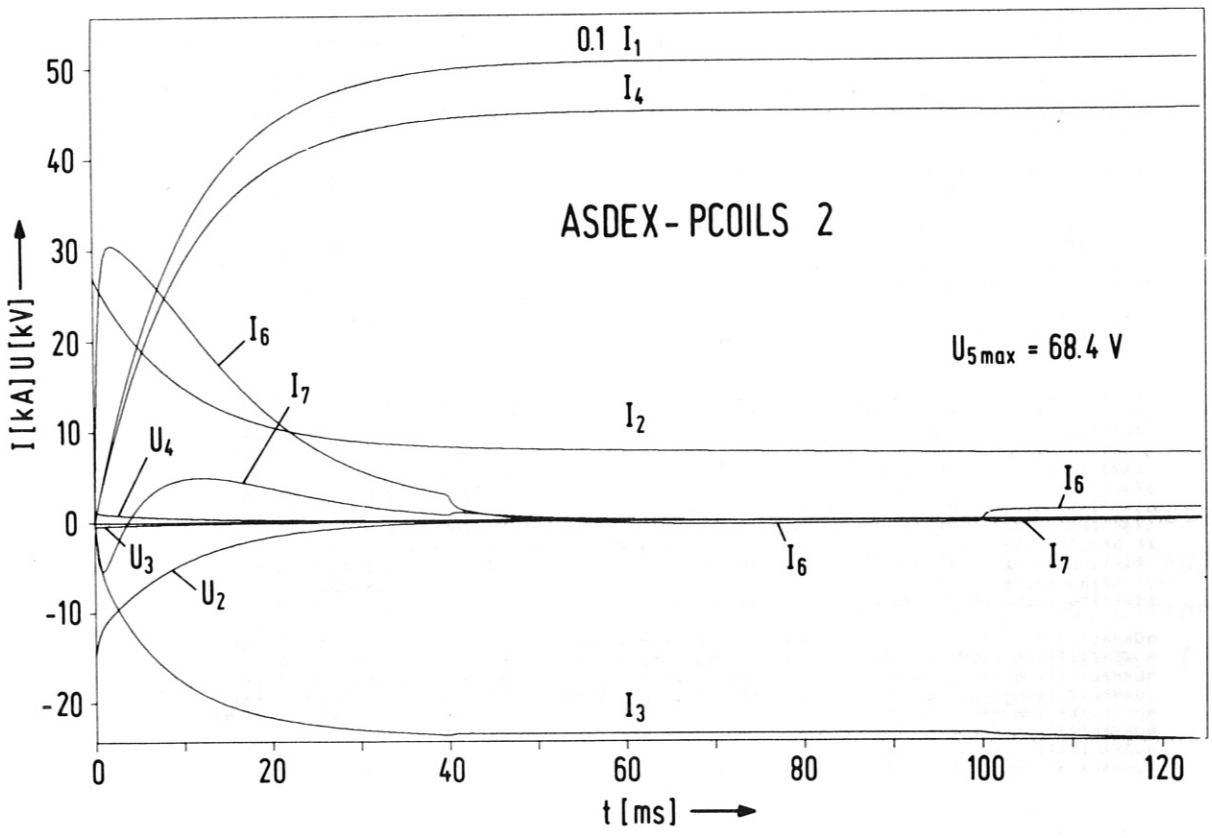
0.1 I1
I4
ASDEX-PCOILS 2
U5max = 68.4 V
I6
I7
I2
U4
I6
U3
I6
I7
U2
I3
I [kA] U [kV]
t [ms]
50
40
30
20
10
0
-10
-20
0
20
40
60
80
100
120

Fig. 13

PCOILS2 INPUT PARAMETERS :
****

NUMBER OF TIME POINTS TO BE CALCULATED	NT	=	312 (-)
NUMBER OF TIME POINTS FOR PRESCRIBED FUNCTION	NTF	=	121 (-)
ISLIT : 0 / 1 -> NO POLOIDAL / POLOIDAL SLIT	ISLIT	=	1
IYOUT : 0 / 1 -> NO OUTPUT / OUTPUT OF Y(T,I) I=1,26	IYOUT	=	1
IBOUT : 0 / 1 -> NO OUTPUT / OUTPUT OF BZ(GR=GRTI,Z=0)	IBOUT	=	1
IPOUT : 0 / 1 -> NO OUTPUT / OUTPUT OF POWERS	IPOUT	=	1
IEOUT : 0 / 1 -> NO OUTPUT / OUTPUT OF ENERGIES	IEOUT	=	1
IAOUT : 0 / 1 -> NO OUTPUT / OUTPUT OF AMPERETURNS AND VOLTAGES PER TURN	IAOUT	=	0
IFOUT : 0 / 1 -> NO OUTPUT / OUTPUT OF FUNCTIONS CALCULATED FROM INPUT	IFOUT	=	1
JINT : RKGS / HPCG -> INTEGRATION BY RUNGE KUTTA / PREDICTOR CORRECTOR	JINT	=	RKGS
ITAB : 0 / 1 -> INPUT FUNCTIONS CALCULATED FROM GIVEN FORMULAE/ INPUT FUNCTIONS CALCULATED FROM TABULATED INPUT	ITAB	=	0
IEIG : 0 / 1 -> NO EIGENVALUE / EIGENVALUE	IEIG	=	0
IFF : 0 / 1 -> NO FEEDFORWARD / FEED FORWARD CONTROL	IFF	=	1
START TIME FOR THE CALCULATION	TO	=	0.0 (S)
TIME STEP FOR THE OUTPUT	DT	=	4.00000E-04 (S)
TIME STEP OF INTEGRATION ROUTINE	DTR	=	1.00000E-04 (S)
NORMALIZATION TIME CHARACTERISTIC OF CURRENT CHANGES	TAUN	=	5.00000E-02 (S)
PLASMA CURRENT FLOW TIME	TAUB	=	1.20000E+00 (S)
TOTAL CYCLE TIME	TAUC	=	1.20000E+00 (S)
ACCURACY LIMIT OF NUMERICAL INTEGRATION PROCEDURE	EPSN	=	1.00000E-04 (-)
CURRENT RAMP UP TIME	TAURU	=	4.00000E-02 (S)
CURRENT RAMP DOWN TIME	TAURD	=	4.00000E-02 (S)
MAGNETIC FIELD AT PLASMA CENTRE	BTRPLO	=	2.80000E+00 (T)
MAJOR RADIUS OF TRANSFORMER COIL CENTRE	GRTR	=	1.69000E+00 (M)
MAJOR RADIUS OF VERTICAL FIELD COIL CENTRE	GRV	=	1.73000E+00 (M)
MAJOR RADIUS OF CENTRAL MAGNETIC LIMITER COIL CENTRE	GRMZ	=	1.65000E+00 (M)
MAJOR RADIUS OF CHAMBER CENTRE	GRC	=	1.65000E+00 (M)
MAJOR RADIUS OF TRANSFORMER INNER EDGE	GRTI	=	8.75000E-01 (M)
MINOR RADIUS OF TRANSFORMER COIL	RTR	=	7.85000E-01 (M)
MINOR RADIUS OF VERTICAL FIELD COIL	RV	=	7.25000E-01 (M)
DISTANCE OF CENTRAL MAGNETIC LIMITER COIL FROM CENTRE	RMZ	=	6.85000E-01 (M)
DISTANCE OF EXCENTRIC MAGNETIC LIMITER COIL FROM CENTRE	RME	=	5.60000E-01 (M)
MINOR CHAMBER RADIUS	RC	=	6.30000E-01 (M)
PLASMA CENTRE SEPARATRIX DISTANCE	RS	=	4.70000E-01 (M)
MINOR Z-HALF HEIGHT OF TRANSFORMER COIL	ZTR	=	1.40000E+00 (M)
MINOR Z-HALF HEIGHT OF VERTICAL FIELD COIL	ZV	=	1.22000E+00 (M)
MINOR Z-HALF HEIGHT OF CHAMBER	ZC	=	1.17000E+00 (M)
THICKNESS OF CHAMBER WALL	DC	=	2.65000E-02 (M)
CROSS SECTIONAL RADIUS OF CENTRAL MAGNETIC LIMITER COIL	RQZ	=	6.35000E-02 (M)
ANGLE BETWEEN R-AXIS AND RMZ	TETAM	=	1.00000E+02 (DEGREE)
ANGLE BETWEEN RMZ AND RME (MAGNETIC LIMITER COILS)	DTETAM	=	2.00000E+01 (DEGREE)
NUMBER OF TURNS , TRANSFORMER COIL	GNTR	=	1.00000E+02 (-)
NUMBER OF TURNS IN ONE CURRENT DIRECTION , VERT. F. COIL	GNV	=	8.00000E+00 (-)
NUMBER OF TURNS , CENTRAL MAGNETIC LIMITER COIL	GNMZ	=	8.00000E+00 (-)
NUMBER OF MAGNETIC LIMITER COIL TRIPLES (0,1,2 OPTIONAL)	NML	=	2.00000E+00 (-)
ELECTRICAL CONDUCTIVITY OF CHAMBER MATERIAL	SIGC	=	9.50000E+05 (1/(OHM*M))
VERTICAL FIELD INDEX	NV	=	1.00000E+00 (-)
IF GRT OR GRVV OR GRML LESS THEN ZERO : PROGRAM CALCULATES RESONABLE ESTIMATES			
RESISTANCE OF TRANSFORMER COIL	GRT	=	1.27000E-02 (OHM)
RESISTANCE OF VERTICAL FIELD COIL	GRVV	=	2.25000E-03 (OHM)
RESISTANCE OF ONE SET OF LIMITER COILS	GRML	=	1.33000E-03 (OHM)
GAIN OF PROPORTIONAL CONTROL	GV	=	1.00000E+01
CHARACTARISTIC TIME OF DIFFERENTIAL CONTROL	TAUD	=	0.0 (S)
CHARACTARISTIC TIME OF INTEGRAL CONTROL	TAUI	=	1.00000E+10 (S)
STARTING VALUE OF NOMINAL MAJOR PLASMA RADIUS GRN	GRNTO	=	1.65000E+00 (M)
STARTING VALUE OF TRANSFORMER CURRENT	ITRTO	=	2.70000E+04 (A)
STARTING VALUE OF SAFETY FACTOR Q	QTO	=	2.71515E+03 (-)
STARTING VALUE OF CHAMBER CURRENT IC0	IC0TO	=	0.0 (A)
STARTING VALUE OF CHAMBER CURRENT IC1	IC1TO	=	0.0 (A)
STARTING VALUE OF CHAMBER CURRENT IC2	IC2TO	=	0.0 (A)
STARTING VALUE OF MINOR PLASMA RADIUS	RPLTO	=	4.07200E-01 (M)
STARTING VALUE OF MAJOR PLASMA RADIUS	GRPLTO	=	1.71000E+00 (M)
IF GRPLTO LESS THEN ZERO : PROGRAM CALCULATES A REASONABLE VALUE FOR GRPLTO			
STARTING VALUE OF REL. INT. PLASMA INDUCTANCE	LITO	=	1.14000E+00 (-)
STARTING VALUE OF POLOIDAL PLASMA BETA	BTPTO	=	1.85700E-03 (-)
STARTING VALUE OF PLASMA ELONGATION RATIO	EPLTO	=	1.00000E+00 (-)
NORMALIZATION VALUE OF PLASMA CURRENT (FLAT TOP VALUE)	IPLO	=	5.00000E+05 (A)
NORMALIZATION VALUE OF SAFETY FACTOR Q (NOMINAL VALUE)	QO	=	2.71515E+00 (-)
NORMALIZATION VALUE OF MAJOR PLASMA RADIUS (NOMINAL VALUE)	GRPLO	=	1.65000E+00 (M)
NORMALIZATION VALUE OF MINOR PLASMA RADIUS (NOMINAL VALUE)	RPLO	=	4.00000E-01 (M)
NORMALIZATION VALUE OF PLASMA RESISTANCE	GRPO	=	1.00000E-06 (OHM)
NORMALIZATION VALUE OF POL. PLASMA BETA (FLAT TOP VALUE)	BETAPO	=	6.50000E-01 (-)
NORMALIZATION VALUE OF REL. INT. PLASMA INDUCTANCE	LIO	=	1.00000E+00 (-)
NORMALIZATION VALUE OF PLASMA ELONGATION	EPLO	=	1.00000E+00 (-)

Table 4

The input functions

$$\dot{q}(t),\ \dot{\beta}_p(t),\ \dot{\ell}_i(t),\ \dot{e}_1(t),\ \dot{R}_n(t),\ \dot{R}_{01}(t)$$

were specified as follows:

$$q(t) = 4q(t)/\tau_{ru}.[(1+q_o/q(o))\, e^{4t/\tau_{ru}}]^{-1} \tag{122}$$

$$\begin{aligned}
\dot{\beta}(t) &= 3.2036 \quad \text{for} \quad t < 0.04\ \text{s} \\
\dot{\beta}_p(t) &= 0 \quad \text{for} \quad 0.04\ \text{s} \leq t < 0.1\ \text{s} \\
\dot{\beta}_p(t) &= 2.600 \quad \text{for} \quad 0.1\ \text{s} \leq t < 0.3\ \text{s} \\
\dot{\beta}_p(t) &= 0 \quad \text{for} \quad t \geq 0.3\ \text{s}
\end{aligned} \tag{123}$$

$$\dot{\ell}_i(t) = 0 \tag{124}$$

$$\dot{e}_1(t) = 0 \tag{125}$$

$$\dot{R}_n(t) = 0 \tag{126}$$

$$\begin{aligned}
R_{01}(t) &\sim 1/I_1(t) \quad \text{for } t < 0.1\ \text{s} \\
R_{01}(t) &= 4.10^{-7}\ \Omega \quad \text{for } t \geq 0.1\ \text{s}\ .
\end{aligned} \tag{127}$$

The corresponding initial values are:

$$\begin{aligned}
q(0) &= 2.71515 \times 10^3 \\
\beta_p(0) &= 1.857 \times 10^{-3} \\
\ell_i(0) &= 1.14 \\
e_1(0) &= 1 \\
R_n(0) &= 1.65\ \text{m}\ .
\end{aligned}$$

The values $q_0 = 2.71515$ and $q(0) = 2.71515 \times 10^3$ correspond to $I_{10} = 5 \times 10^5$ A, $I_1(0) = 5 \times 10^2$ A. With these values for q_0 and $q(0)$ the integration of eq. (122) leads to a $q(t)$ which would exactly correspond to $I_1(t)$ resulting from eq. (115) if $\dot{R}_1(t)$ were 0. Because in PCOILS 2 $\dot{R}_n(t)$ is given and $R_1(t)$ is feedback controlled, differences between $I_1(t)$ from eq. (115) and $I_1(t)$ corresponding to eq. (122) occur as long as $R_1(t)$ has not become equal to $R_n(t) = R_n(0)$.

The voltage U_3 applied to the vertical field coil is given by

$$U_3 = U_{3ff} + U_{3fb} \cdot \tag{128}$$

The feed-forward component U_{3ff} is specified as follows:

$$U_{3ff} = L_3 \dot{I}_{3n} + (M_{13n} I_{1n})^{\cdot} + R_3 I_{3n} \ , \tag{129}$$

$$I_{3n} = \nu_{1n}/\nu_3 \cdot I_{1n} \ . \tag{130}$$

The index "n" in eqs. (129) and (130) means "nominal", i.e. the parameters are calculated by using the prescribed functions $q(t)$, $\beta_p(t)$, $\ell_i(t)$, $e_1(t)$, $R_n(t)$. I_{1n} follows from q via eq. (30). Thus, U_{3ff} is completely determined by given functions and parameters.

The feedback voltage U_{3fb} is given by

$$U_{3fb} = -I_{3n} R_3 / R_{1o} \cdot G \ (R_n - R_1) \ , \tag{131}$$

which follows from eq. (94) for $U_{3n} = I_{3n} R_3$, $\tau_d = 0$, $\tau_i \rightarrow \infty$. R_{1O} is a normalization value for the major plasma radius R_1. Here $R_{1O} = R_n(0) = 1.65$ has been chosen. U_{3fb} according to eq. (131) describes a proportional control.

Figure 13 corresponds to Fig. 12 and shows the various currents and voltages as functions of time for the gain G = 10. Figure 14 shows the given functions $R_n(t)$ and $\beta_p(t)$ together with $R_1(t)$, $r_1(t)$ and $B_z(t)$.

Comparison of Figs. 12 and 13 shows that they deviate from each other practically only with respect to the dipole and quadrupole chamber currents I_6 and I_7. They are considerably larger for PCOILS 2 than for PCOILS 1. Because of the strong influence of I_6 on the plasma position this means that PCOILS 2 has to be used if control voltages and powers are an important issue. The overall energy balance, on the other hand, is practically not changed: I_6 and I_7 in PCOILS 2 dissipate 6.52 kJ during the first 125 ms, which is small compared with, for

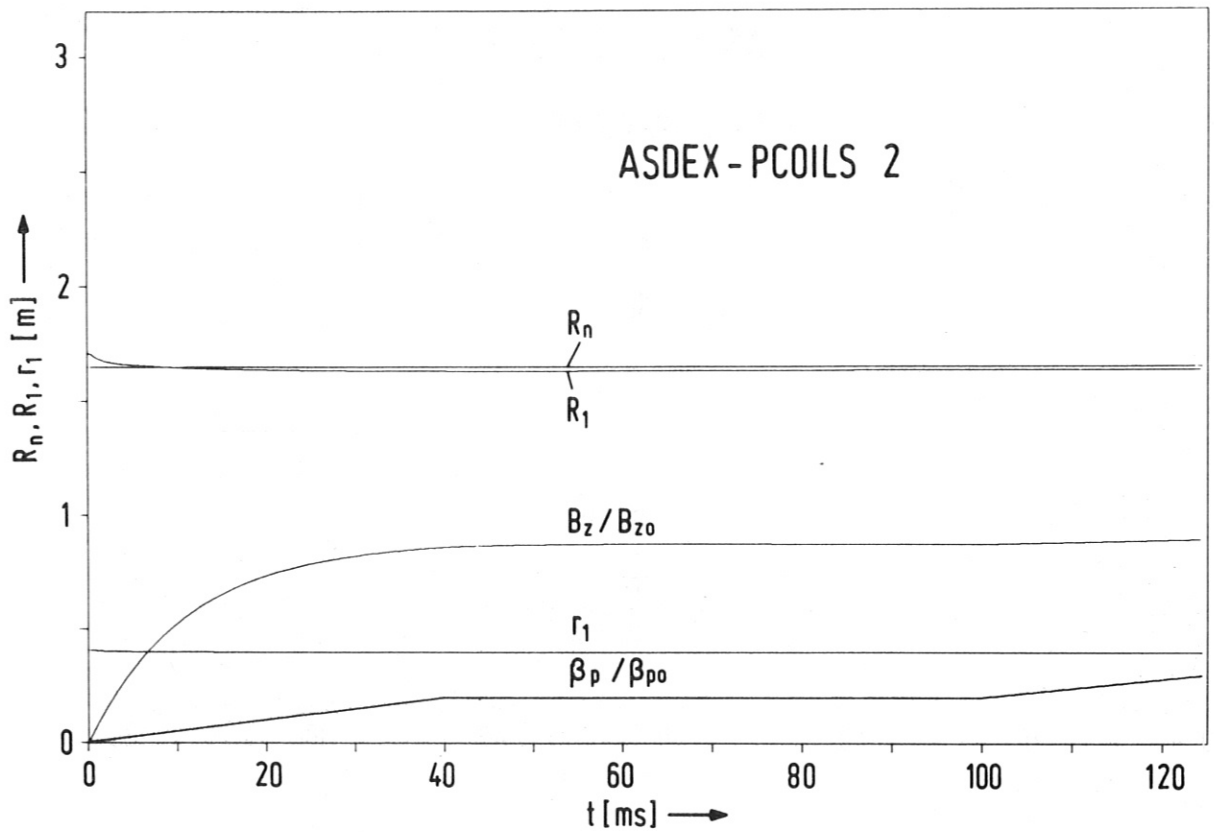

Fig. 14

example, the ohmic losses of 931.6 MJ in the remaining coils. Because, furthermore, the relative importance of the energy dissipated in the chamber walls decreases with increasing plasma current flow time, the PCOILS 1 model is sufficient for studying energy balances, as already anticipated at the beginning of Sec. 5.1.

For comparison we also calculated the following cases:

a) $U_{3ff} = 0$, $U_{3fb} = 0$, i.e. neither feedforward nor feedback control.

b) $U_{3ff} = 0$, U_{3fb} according to eq. (131) with G = 10, i.e. feedback control only.

c) U_{3ff} according to eq. (129), $U_{3fb} = 0$; i.e. feedforward control only.

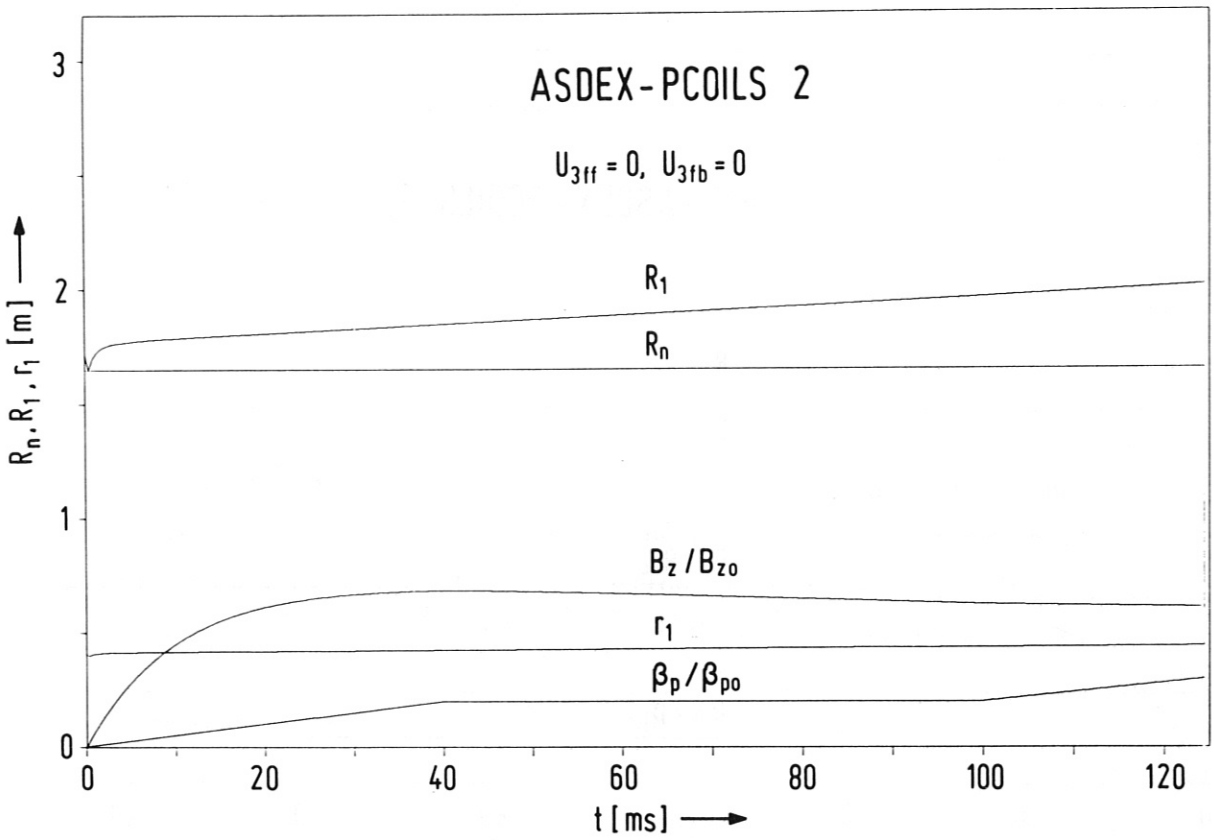

Fig. 15

Figure 15, which shows $R_1(t)$, $r_1(t)$, $\beta_p(t)$, and $B_z(t)$ for case a) ($U_{3ff} = 0$, $U_{3fb} = 0$) demonstrates that shortly after the start of the current rise the column begins to move slowly towards larger major radii. The velocity of this movement is governed by the currents I_3 and I_6 (see Fig. 16). During the initial phase both $\dot{I}_1$ and $\dot{R}_1$ (via M_{13} and M_{16}) drive I_3 and I_6, whereas during the flat-top phase of I_1 only the influence of $\dot{R}_1$ persists, which leads to practically constant values of I_3 and I_6. The case considered demonstrates the partial, passive stabilization of the plasma position by induction of dipole currents in the chamber and the vertical field coils.

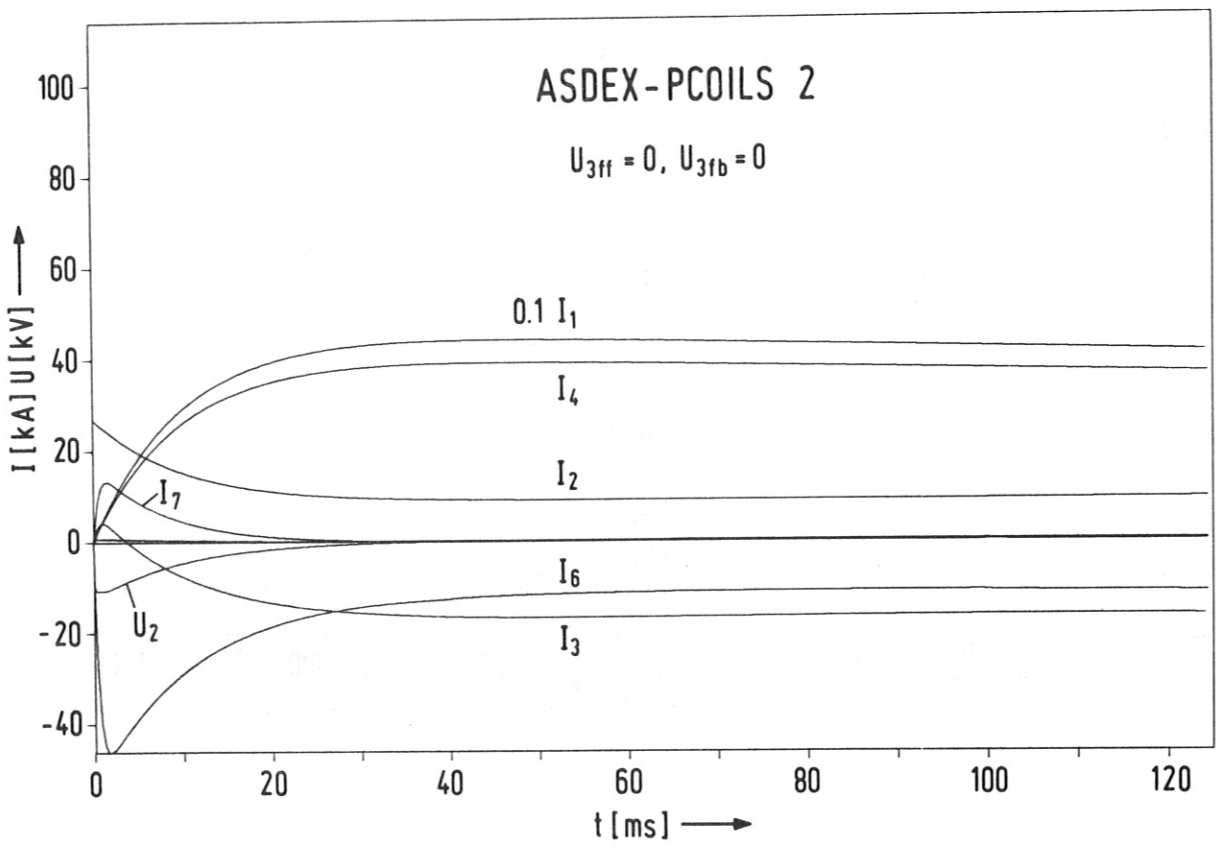

Fig. 16

The pure feedback control (case b)) is demonstrated by Figs. 17 and 18. Figure 17 shows that R_1 reaches a stationary value after a short dynamic phase. The difference $\Delta R_1 = R_1 - R_n$ then obeys the relation $\Delta R_1/R_1 \approx 1/G$, which is typical of proportional control.

Figure 19 demonstrates that feedforward control alone (case c)) already leads to small deviations of R_1 from the nominal value R_n. Figure 20 shows the corresponding currents and voltages.

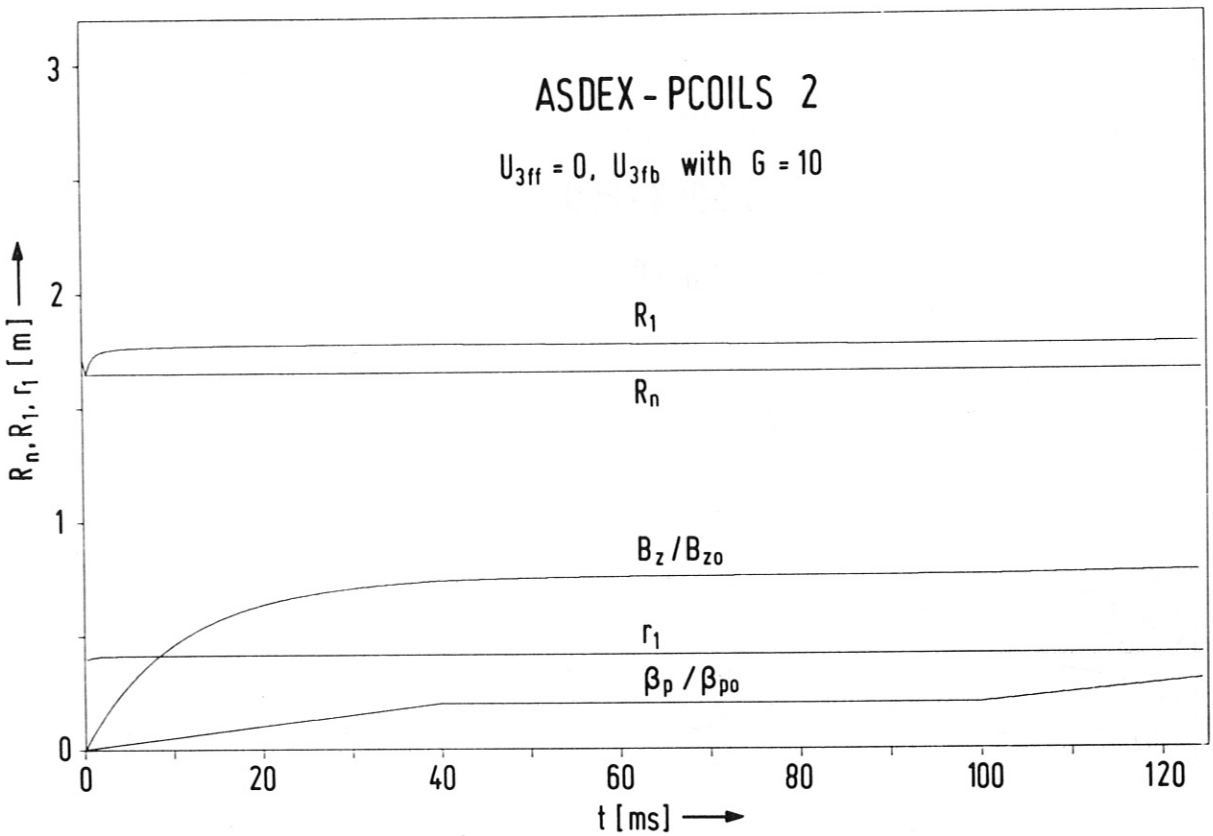
ASDEX - PCOILS 2
$U_{3ff} = 0$, U_{3fb} with G = 10
R_n, R_1, r_1 [m]
R_1
R_n
B_z / B_{zo}
r_1
β_p / β_{po}
t [ms]

Fig. 17

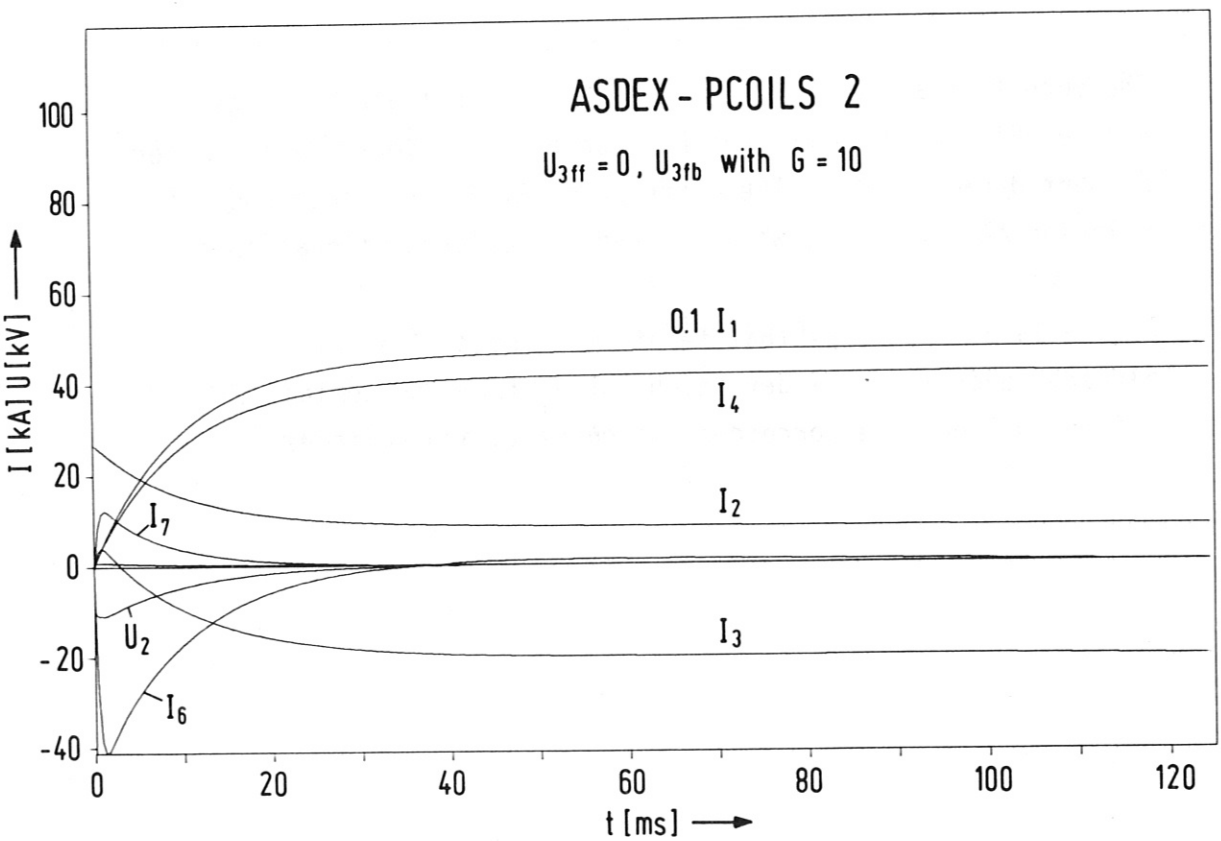
ASDEX - PCOILS 2
$U_{3ff} = 0$, U_{3fb} with G = 10
I [kA] U [kV]
0.1 I_1
I_4
I_2
I_7
I_3
U_2
I_6
t [ms]

Fig. 18

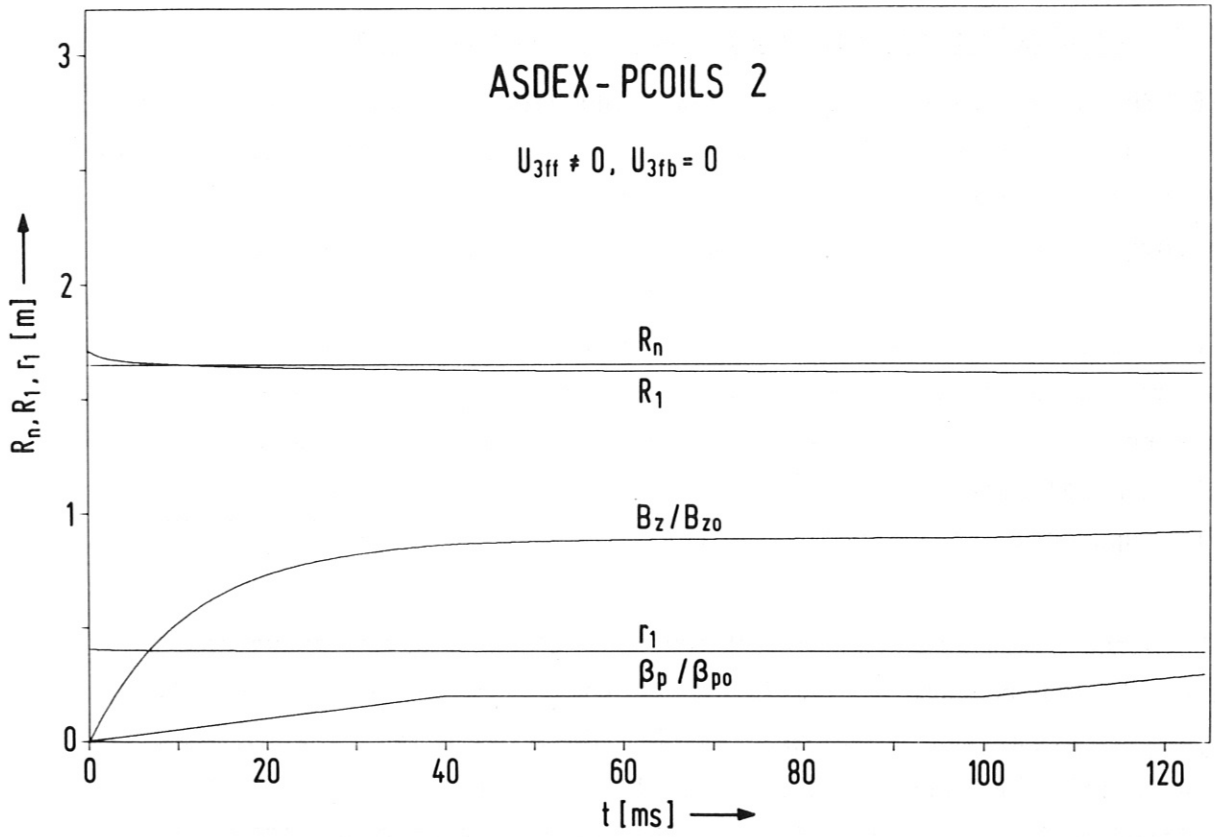
ASDEX - PCOILS 2
$U_{3ff} \neq 0$, $U_{3fb} = 0$
R_n, R_1, r_1 [m]
R_n
R_1
B_z / B_{zo}
r_1
β_p / β_{po}
t [ms]

Fig. 19

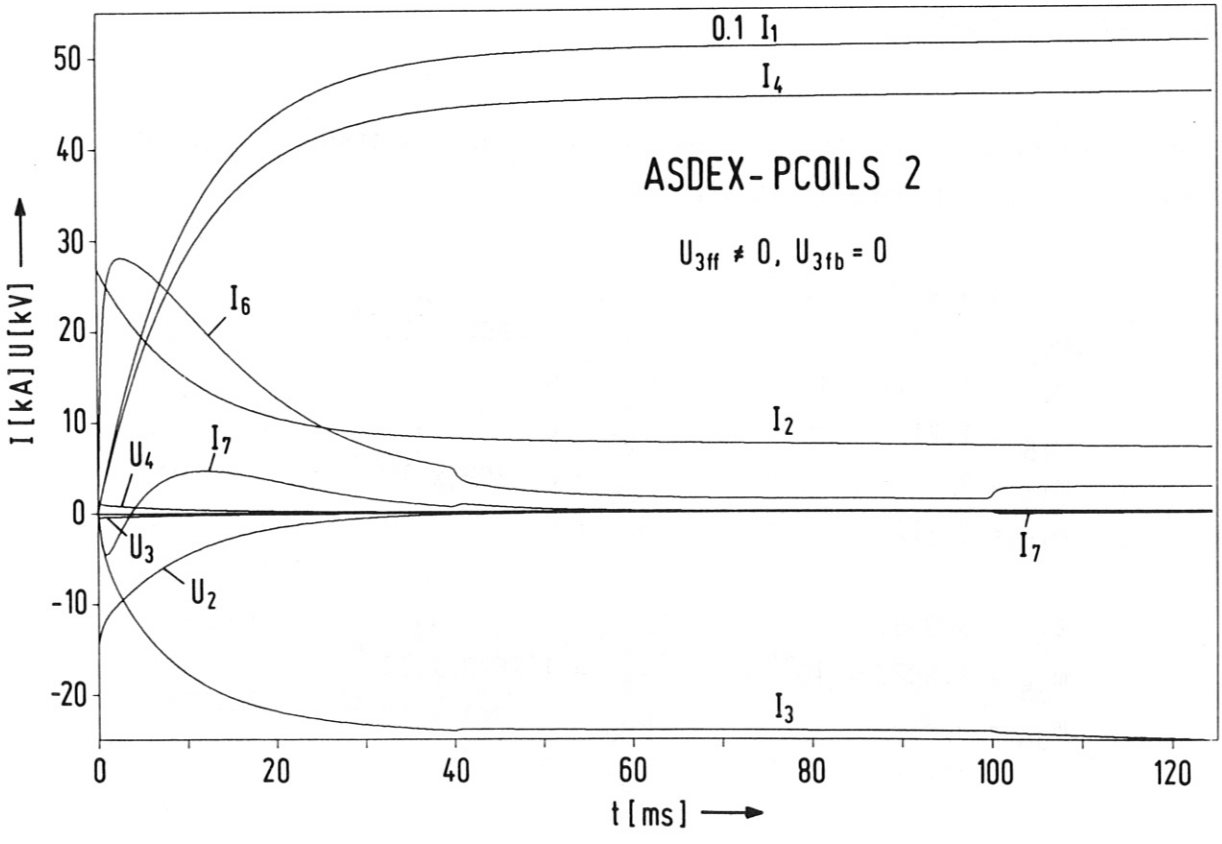
ASDEX - PCOILS 2
$U_{3ff} \neq 0$, $U_{3fb} = 0$
I [kA] U [kV]
0.1 I_1
I_4
I_6
I_2
I_7
U_4
I_7
U_3
U_2
I_3
t [ms]

Fig. 20

6.2 Calculations for the ZEPHYR compression experiment

ZEPHYR is a tokamak experiment now being discussed and planned at IPP. A major feature of ZEPHYR is the compression of the major plasma radius R_1 by a factor of about 1.5 within 50 ms. This decrease of R_1 is accomplished by an increase of the vertical magnetic field B_z.

To investigate the compression phase with PCOILS 2, we assume that the plasma has already reached a stationary phase by ohmic heating before compression starts. Compression is initiated by a sudden decrease of the nominal major radius R_n from its previous value of 2.03 m to 1.35 m. The input data is listed in Table 5.

The numbers for TAURU and TAURD are only formal and not actually used because no external variation of the plasma current I_1 (expressed by $\dot{q}$) is assumed. The numbers for RMZ, RME, RS, TETAM, DTETAM, GRML are formal, too, because they refer to divertor triples which are omitted by NML = 0. The values of the transformer and vertical field coil resistances (GRT, GRVV) are estimates based on eqs. (64) and (66). The numbers of turns in the various coils of the experiment have not yet been specified. We therefore set the numbers of turns equal to unity, which means that the program yields ampere-turns and voltages per turns as results.

The inductances, magnetic field parameters, and resistances calculated from the input data are as follows (MKSA units):

$$\ell_1 = 4.1348 \times 10^{-6}$$
$$m_{12} = 7.2928 \times 10^{-7} \qquad \ell_2 = 1.6862 \times 10^{-7}$$
$$m_{13} = 1.9011 \times 10^{-6} \qquad m_{23} = 0$$
$$m_{15} = 1.7175 \times 10^{-6} \qquad m_{25} = 0$$
$$m_{16} = 3.6498 \times 10^{-6} \qquad m_{26} = 8.4309 \times 10^{-8}$$
$$m_{17} = 1.7175 \times 10^{-6} \qquad m_{27} = 0$$

$$\ell_3 = 3.9960 \times 10^{-6}$$
$$m_{35} = 1.5820 \times 10^{-6} \qquad \ell_5 = 1.2673 \times 10^{-6}$$
$$m_{36} = 3.4135 \times 10^{-6} \qquad m_{56} = 2.1941 \times 10^{-6}$$
$$m_{37} = -1.6726 \times 10^{-6} \qquad m_{57} = 0$$

```
PCOILS2 INPUT PARAMETERS :
**************************

NUMBER OF TIME POINTS TO BE CALCULATED                          NT    =          125 (-)
NUMBER OF TIME POINTS FOR PRESCRIBED FUNCTION                   NTF   =            6 (-)

ISLIT : 0 / 1 -> NO POLOIDAL / POLOIDAL SLIT                    ISLIT =            1
IYOUT : 0 / 1 -> NO OUTPUT / OUTPUT OF Y(T,I)  I=1,26           IYOUT =            1
IBOUT : 0 / 1 -> NO OUTPUT / OUTPUT OF BZ(GR=GRTI,Z=0)          IBOUT =            1
IPOUT : 0 / 1 -> NO OUTPUT / OUTPUT OF POWERS                   IPOUT =            1
IEOUT : 0 / 1 -> NO OUTPUT / OUTPUT OF ENERGIES                 IEOUT =            1
IAOUT : 0 / 1 -> NO OUTPUT / OUTPUT OF AMPERETURNS AND
                  VOLTAGES PER TURN                             IAOUT =            1
IFOUT : 0 / 1 -> NO OUTPUT / OUTPUT OF FUNCTIONS CALCULATED
                  FROM INPUT                                    IFOUT =            1
JINT : RKGS / HPCG -> INTEGRATION BY
          RUNGE KUTTA / PREDICTOR CORRECTOR                     JINT  =      RKGS
ITAB : 0 / 1 -> INPUT FUNCTIONS CALCULATED FROM GIVEN
FORMULAE/ INPUT FUNCTIONS CALCULATED FROM TABULATED INPUT       ITAB  =            1
IEIG : 0 / 1 -> NO EIGENVALUE / EIGENVALUE                      IEIG  =            0
IFF  : 0 / 1 -> NO FEEDFORWARD / FEED FORWARD CONTROL           IFF   =            1

START TIME FOR THE CALCULATION                                  T0    =    0.0           (S)
TIME STEP FOR THE OUTPUT                                        DT    =    1.00000E-03 (S)
TIME STEP OF INTEGRATION ROUTINE                                DTR   =    1.00000E-04 (S)

NORMALIZATION TIME CHARACTERISTIC OF CURRENT CHANGES            TAUN  =    1.00000E-01 (S)
PLASMA CURRENT FLOW TIME                                        TAUB  =    5.00000E+00 (S)
TOTAL CYCLE TIME                                                TAUC  =    5.00000E+00 (S)

ACCURACY LIMIT OF NUMERICAL INTEGRATION PROCEDURE               EPSN  =    1.00000E-04 (-)

CURRENT RAMP UP TIME                                            TAURU =    5.00000E-01 (S)
CURRENT RAMP DOWN TIME                                          TAURD =    5.00000E-03 (S)

MAGNETIC FIELD AT PLASMA CENTRE                                 BTRPLO=    6.09000E+00 (T)

MAJOR RADIUS OF TRANSFORMER COIL CENTRE                         GRTR  =    1.94000E+00 (M)
MAJOR RADIUS OF VERTICAL FIELD COIL CENTRE                      GRV   =    2.00000E+00 (M)
MAJOR RADIUS OF CENTRAL MAGNETIC LIMITER COIL CENTRE            GRMZ  =    2.00000E+00 (M)
MAJOR RADIUS OF CHAMBER CENTRE                                  GRC   =    1.76000E+00 (M)
MAJOR RADIUS OF TRANSFORMER INNER EDGE                          GRTI  =    1.00000E-01 (M)

MINOR RADIUS OF TRANSFORMER COIL                                RTR   =    1.70000E+00 (M)
MINOR RADIUS OF VERTICAL FIELD COIL                             RV    =    1.40000E+00 (M)
DISTANCE OF CENTRAL MAGNETIC LIMITER COIL FROM CENTRE           RMZ   =    8.00000E-01 (M)
DISTANCE OF EXCENTRIC MAGNETIC LIMITER COIL FROM CENTRE         RME   =    6.50000E-01 (M)
MINOR CHAMBER RADIUS                                            RC    =    9.60000E-01 (M)
PLASMA CENTRE SEPARATRIX DISTANCE                               RS    =    5.50000E-01 (M)

MINOR Z-HALF HEIGHT OF TRANSFORMER COIL                         ZTR   =    1.43000E+00 (M)
MINOR Z-HALF HEIGHT OF VERTICAL FIELD COIL                      ZV    =    1.43000E+00 (M)
MINOR Z-HALF HEIGHT OF CHAMBER                                  ZC    =    7.40000E-01 (M)

THICKNESS OF CHAMBER WALL                                       DC    =    1.00000E-02 (M)
CROSS SECTIONAL RADIUS OF CENTRAL MAGNETIC LIMITER COIL         RQZ   =    6.35000E-02 (M)

ANGLE BETWEEN R-AXIS AND RMZ                                    TETAM =    9.00000E+01 (DEGREE)
ANGLE BETWEEN RMZ AND RME (MAGNETIC LIMITER COILS)              DTETAM=    2.00000E+01 (DEGREE)

NUMBER OF TURNS , TRANSFORMER COIL                              GNTR  =    1.00000E+00 (-)
NUMBER OF TURNS IN ONE CURRENT DIRECTION  , VERT. F. COIL       GNV   =    1.00000E+00 (-)
NUMBER OF TURNS , CENTRAL MAGNETIC LIMITER COIL                 GNMZ  =    1.00000E+00 (-)
NUMBER OF MAGNETIC LIMITER COIL TRIPLES (0,1,2 OPTIONAL)        NML   =    0.0         (-)
ELECTRICAL CONDUCTIVITY OF CHAMBER MATERIAL                     SIGC  =    7.69000E+05 (1/(OHM*M))
VERTICAL FIELD INDEX                                            NV    =    1.00000E+00 (-)

IF GRT OR GRVV OR GRML LESS THEN ZERO : PROGRAM CALCULATES RESONABLE ESTIMATES
RESISTANCE OF TRANSFORMER COIL                                  GRT   =    1.20731E-07 (OHM)
RESISTANCE OF VERTICAL FIELD COIL                               GRVV  =    6.35370E-06 (OHM)
RESISTANCE OF ONE SET OF LIMITER COILS                          GRML  =    0.0         (OHM)

GAIN OF PROPORTIONAL CONTROL                                    GV    =    1.00000E+01
CHARACTARISTIC TIME OF DIFFERENTIAL CONTROL                     TAUD  =    0.0         (S)
CHARACTARISTIC TIME OF INTEGRAL CONTROL                         TAUI  =    1.00000E+10 (S)

STARTING VALUE OF NOMINAL MAJOR PLASMA RADIUS GRN               GRNTO =    2.03000E+00 (M)
STARTING VALUE OF TRANSFORMER CURRENT                           ITRTO =    0.0         (A)
STARTING VALUE OF SAFETY FACTOR Q                               QTO   =    2.53699E+00 (-)
STARTING VALUE OF CHAMBER CURRENT IC0                           ICOTO =    0.0         (A)
STARTING VALUE OF CHAMBER CURRENT IC1                           IC1TO =    0.0         (A)
STARTING VALUE OF CHAMBER CURRENT IC2                           IC2TO =    0.0         (A)
STARTING VALUE OF MINOR PLASMA RADIUS                           RPLTO =    6.10000E-01 (M)
STARTING VALUE OF MAJOR PLASMA RADIUS                           GRPLTO=    2.03000E+00 (M)
IF GRPLTO LESS THEN ZERO : PROGRAM CALCULATES A REASONABLE VALUE FOR GRPLTO
STARTING VALUE OF REL. INT. PLASMA INDUCTANCE                   LITO  =    1.08000E+00 (-)
STARTING VALUE OF POLOIDAL PLASMA BETA                          BTPTO =    1.20000E+00 (-)
STARTING VALUE OF PLASMA ELONGATION RATIO                       EPLTO =    1.00000E+00 (-)

NORMALIZATION VALUE OF PLASMA CURRENT (FLAT TOP VALUE)          IPLO  =    2.20000E+06 (A)
NORMALIZATION VALUE OF SAFETY FACTOR Q (NOMINAL VALUE)          QO    =    2.53700E+00 (-)
NORMALIZATION VALUE OF MAJOR PLASMA RADIUS (NOMINAL VALUE)GRPLO =    2.03000E+00 (M)
NORMALIZATION VALUE OF MINOR PLASMA RADIUS (NOMINAL VALUE)RPLO  =    6.10000E-01 (M)
NORMALIZATION VALUE OF PLASMA RESISTANCE                        GRPO  =    1.00000E-07 (OHM)
NORMALIZATION VALUE OF POL. PLASMA BETA (FLAT TOP VALUE)        BETAPO=    1.00000E+00 (-)
NORMALIZATION VALUE OF REL. INT. PLASMA INDUCTANCE              LIO   =    1.00000E+00 (-)
NORMALIZATION VALUE OF PLASMA ELONGATION                        EPLO  =    1.00000E+00 (-)
```

Table 5

$$\ell_6 = 5.4571 \times 10^{-6}$$
$$m_{67} = 2.2325 \times 10^{-6} \qquad \ell_7 = 1.0914 \times 10^{-5}$$

$$\nu_1 = -1.6166 \times 10^{-7}$$
$$\nu_{21}/N_2 = 0$$
$$\nu_{31}/N_3 = 1.8013 \times 10^{-7}$$
$$\nu_{51} = 1.2418 \times 10^{-7}$$
$$\nu_{61} = 3.2725 \times 10^{-7}$$
$$\nu_{71} = 2.7333 \times 10^{-7}$$

$$R_{05} = 2.3841 \times 10^{-4}$$
$$R_{06} = 1.1765 \times 10^{-3}$$
$$R_{07} = 4.7059 \times 10^{-3}$$

L/R times calculated from these values, from the normalization value $R_{010} = 10^{-7}\ \Omega$ of the plasma resistance, and from the given R_{02}, R_{03} are:

$$L_1/R_{010} = 4.1348 \times 10^{1}\ s$$
$$L_2/R_{02} = 1.3967\ s$$
$$L_3/R_{03} = 6.2893 \times 10^{-1}\ s$$
$$L_5/R_{05} = 5.3159 \times 10^{-3}\ s$$
$$L_6/R_{06} = 4.6385 \times 10^{-3}\ s$$
$$L_7/R_{07} = 2.3193 \times 10^{-3}\ s\ .$$

The input functions are specified as follows:

$$\dot{q}(t) = 0 \tag{132}$$
$$\dot{\beta}_p(t) = 0 \tag{133}$$
$$\dot{\ell}_i(t) = 0 \tag{134}$$
$$\dot{e}_1(t) = 0 \tag{135}$$

$$\begin{aligned} \dot{R}_n(t) &= 0 \quad \text{for} \quad t < 2.5 \times 10^{-2}\ s \\ \dot{R}_n(t) &= -13.6\ m/s \quad \text{for} \quad 2.5 \times 10^{-2}\ s \leq t \leq 7.5 \times 10^{-2}\ s \\ \dot{R}_n(t) &= 0 \quad \text{for} \quad t > 7.5 \times 10^{-2}\ s \end{aligned} \tag{136}$$

$$R_{01}(t) = \text{const} = 10^{-7}\ \Omega \tag{137}$$

The corresponding initial values are:

$$q(0) = 2.537$$
$$\beta_p(0) = 1.2$$
$$\ell_i(0) = 1.08$$
$$e_1(0) = 1$$
$$R_n(0) = 2.03 \text{ m}.$$

The preceding data implies that q, β_p, ℓ_i, and e_1 remain constant during compression, which means that the zero-order relationship $\beta_p \overset{\sim}{\propto} R_1^{-1/3}$ is ignored. The value $q = 2.537$ corresponds to the nominal values of R_1, I_1, and B_t during the precompression phase if we set $q(r_1 = 0) = 1$. The ratio $q/q(r_1 = 0) = 2.537$ is valid for the profile exponent $n = 1.537$ used in eq. (44), which, in turn, leads to $\ell_i = 1.08$ (see Fig. 6).

The feedforward and feedback voltages U_{3ff} and U_{3fb} are again given by eqs. (129) and (131).

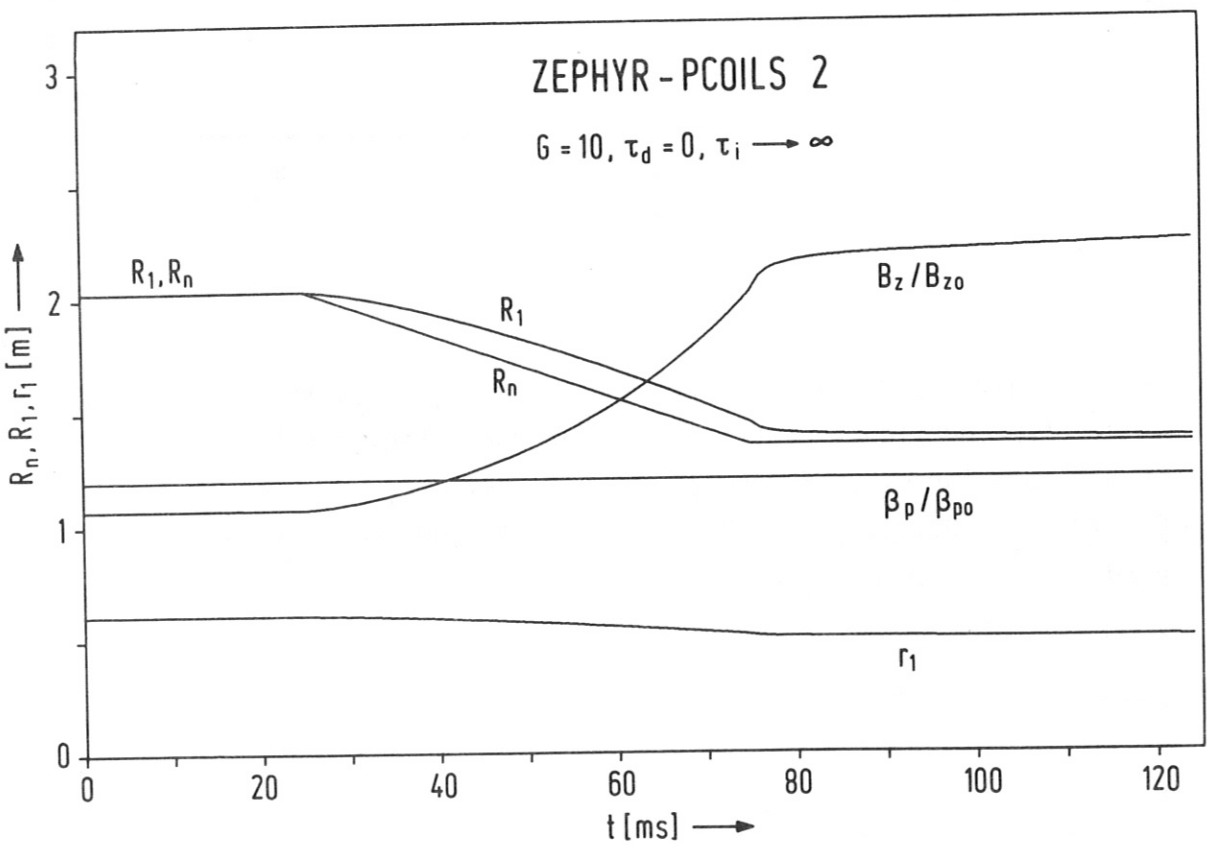

Fig. 21

Figure 21 shows R_n together with R_1, r_1, B_z, and β_p for $G = 10$.

The response of R_1 to the variation of R_n can be made more favourable by using a differential contribution to the feedback voltage U_{3fb}. This is accomplished by using eq. (94) for U_{3fb} with G = 10, τ_d = 0.1 s, $\tau_i \longrightarrow \infty$. Figure 22 shows the results.

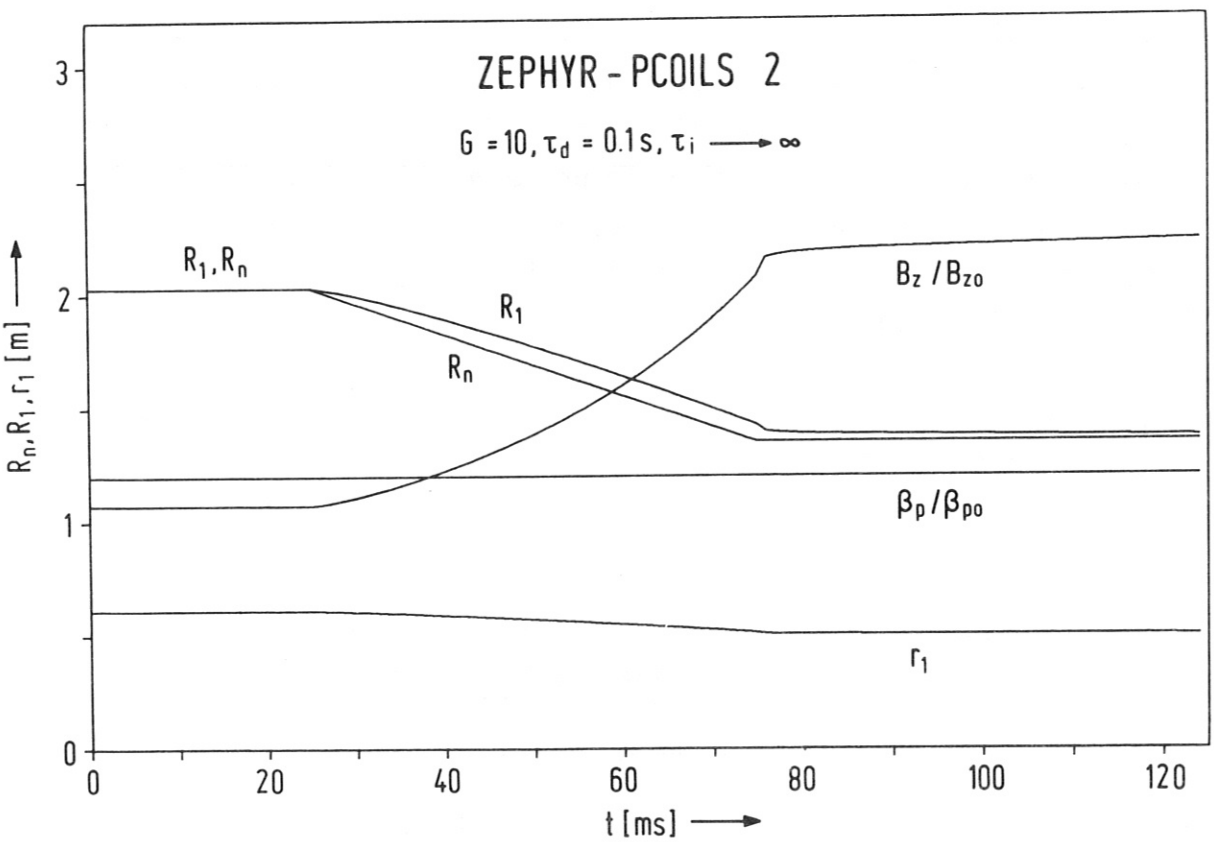

Fig. 22

To eliminate the remaining difference $\Delta R_1 = R_1 - R_n$, which is characteristic of proportional control, one can use a finite value for τ_i in eq. (94) for U_{3fb}. Figure 23 shows R_n, R_1, r_1, B_z, and β_p for G = 10, τ_d = 0.1 s, τ_i = 0.03 s. Figure 24 shows some of the corresponding ampere-turns $A_i = N_i I_i$.

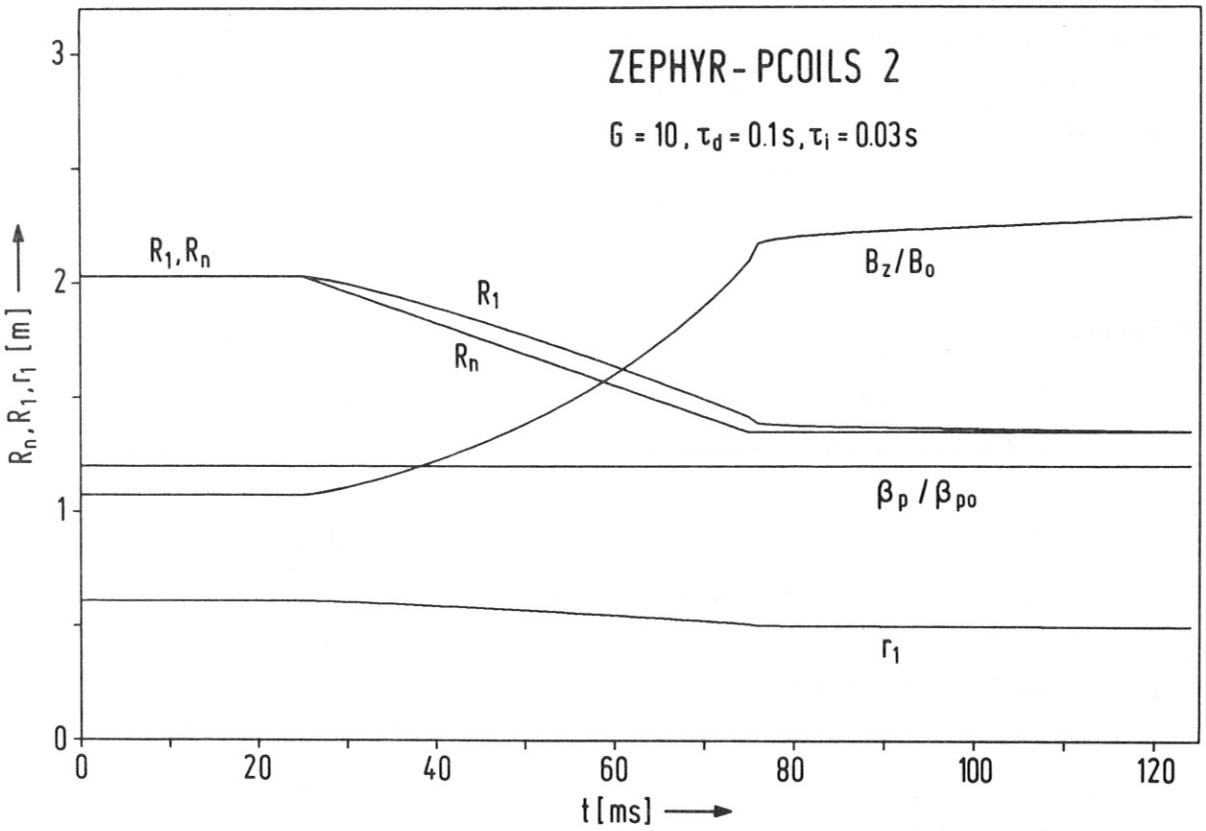
ZEPHYR-PCOILS 2
G = 10, τd = 0.1s, τi = 0.03s
R1, Rn
R1
Rn
Bz/Bo
βp / βpo
r1
Rn, R1, r1 [m]
t [ms]
0
20
40
60
80
100
120
1
2
3

Fig. 23

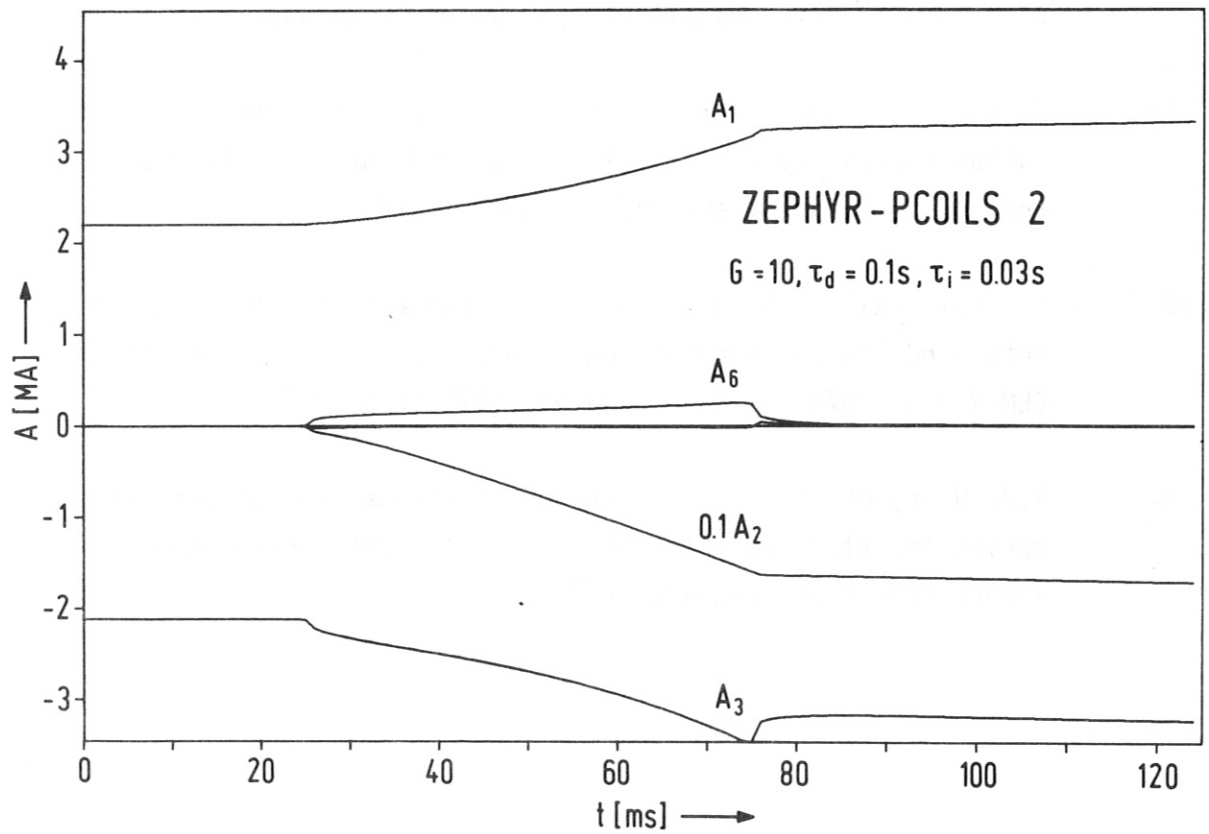
ZEPHYR-PCOILS 2
G = 10, τd = 0.1s, τi = 0.03s
A1
A6
0.1 A2
A3
A [MA]
t [ms]
0
20
40
60
80
100
120
4
3
2
1
-1
-2
-3

Fig. 24

Acknowledgements

The authors greatly appreciate the many discussions held with K. Borrass and F. Schneider as well as the assistance of H. Preis and P. Martin in numerically calculating ASDEX inductances to check the analytical results.

References

/1/ V.S. Mukhovatov, V.D. Shafranov: "Plasma equilibrium in a tokamak", Nucl. Fus., 11 (1971), 605.

/2/ Y. Suzuki et al.: "Tokamak circuit theory", JAERI-Report JAERI-M 6531, 1976 (Culham translation CTO/1449).

/3/ J. Raeder: "A mathematical model of the pulsed coil system of a tokamak reactor", IPP-Report IPP 4/174, January 1979.

/4/ F.W. Grover: "Inductance calculations: working formulas and tables", Dover Publications, In., New York, 1962.

/5/ J.H. Malmberg, M.N. Rosenbluth: "High frequency inductance of a torus", Rev. Scient. Instrum., 36, 12 (1965), 1886.

/6/ K. Khalaf-Allah: "Eddy current loss in pulsed magnetic fields", Culham Laboratory report CLM-R 139, 1974. We refer to the analysis on page 4, especially to eq. (2-4).

/7/ K. Khalaf-Allah: "Time constant for magnetic field diffusion into a hollow cylindrical conductor", Culham Laboratory report CLM-R 141, 1974. We have used eq. (22) on page 5.

/8/ R.J. Hawryluk, K. Bol, D. Johnson: "Volt-second consumption during the start up phase of a large tokamak", Princeton Report PPPL-1508, January 1979.

/9/ L.D. Landau, E.M. Lifshitz: "Electrodynamics of continuous media", volume 8 of the course of theoretical physics, Pergamon Press, Oxford, London, New York, Paris, 1963.

/10/ M. Abramowitz, I.A. Stegun, ed.: "Handbook of mathematical functions", Dover Publications, Inc., New York, 1965, p.591.

/11/ K. Borrass: "A zero dimensional tokamak transport model. Part I - General description", IPP-Report IPP 4/146, 1977.

/12/ K. Borrass, R. Buende, W. Daenner: "First results with the SISYFUS code: The influence of plasma impurities on the performance of tokamak power plants", 3rd Topical Meeting on the Technology of Controlled Thermonuclear Fusion, Santa Fé,N.M., 1978.

/13/ K. Borrass, R. Buende, W. Daenner: "SISYFUS - A simulation model for systematic analyses of fusion power plants", 10th Symposium on Fusion Technology, Padua, Italy, 1978.

/14/ K. Borrass, R. Buende, W. Daenner, H. Gorenflo, J. Raeder, M. Soell: "Scoping studies for the layout of a low power tokamak experimental fusion power plant on the basis of empirical scaling", 8th Symposium on Engineering Problems of Fusion Research, San Francisco, Ca., Nov. 1979.

/15/ K. Borrass, K. Lackner, E. Minardi: "Direct energy conversion and control of unstable burn by cyclic major radius compression and decompression", 9th Europ. Conference on Controlled Fusion and Plasma Physics, Oxford, U.K., Sept. 1979.